A finite difference Hartree-Fock program for atoms and diatomic molecules

Jacek Kobus

Instytut Fizyki, Uniwersytet Mikołaja Kopernika, Grudziądzka 5, 87-100 Toruń, Poland

Abstract

The newest version of the two-dimensional finite difference Hartree-Fock program for atoms and diatomic molecules is presented. This is an updated and extended version of the program published in this journal in 1996. It can be used to obtain reference, Hartree-Fock limit values of total energies and multipole moments for a wide range of diatomic molecules and their ions in order to calibrate existing and develop new basis sets, calculate (hyper)polarizabilities (α_{zz}, β_{zzz}, γ_{zzzz}, $A_{z,zz}$, $B_{zz,zz}$) of atoms, homonuclear and heteronuclear diatomic molecules and their ions via the finite field method, perform DFT-type calculations using LDA or B88 exchange functionals and LYP or VWN correlations ones or the self-consistent multiplicative constant method, perform one-particle calculations with (smooth) Coulomb and Krammers-Henneberger potentials and take account of finite nucleus models. The program is easy to install and compile (tarball+configure+make) and can be used to perform calculations within double- or quadruple-precision arithmetic.

Keywords: Schrödinger equation of one-electron atomic and diatomic systems, restricted open-shell Hartree-Fock method, atoms, diatomic molecules, density functional theory potentials, Gauss and Fermi nuclear charge distributions, finite field method, prolate spheroidal coordinates, 8th-order discretization, (multicolour) successive overrelaxation
2000 MSC: 35Q40, 65N06, 65N22, 81V45, 81V55

NEW VERSION PROGRAM SUMMARY

Manuscript Title: A finite difference Hartree-Fock program for atoms and diatomic molecules
Authors: Jacek Kobus

Program Title: 2dhf
Journal Reference:
Catalogue identifier:
Licensing provisions: GPL
Programming language: Fortran 77, C
Computer: any 32- or 64-bit platform
Operating system: Unix/Linux
RAM: case dependent, from few MB to many GB
Number of processors used:
Supplementary material:
Keywords: restricted open-shell Hartreee-Fock method, DFT potentials, prolate spheroidal coordinates, 8th-order discretization, (multicolour) successive overrelaxation method,
Classification: 16.1
External routines/libraries:
Subprograms used:
*Catalogue identifier of previous version: ADEB_v1_0**
*Journal reference of previous version: Comput. Phys. Commun. 98(1996)346**
*Does the new version supersede the previous version?: yes**

Nature of problem: The program finds virtually exact solutions of the Hartree-Fock and density functional theory type equations for atoms, diatomic molecules and their ions. The lowest energy eigenstates of a given irreducible representation and spin can be obtained. The program can be used to perform one-particle calculations with (smooth) Coulomb and Krammers-Henneberger potentials and also DFT-type calculations using LDA or B88 exchange functionals and LYP or VWN correlations ones or the self-consistent multiplicative constant method.

Solution method: Single-particle two-dimensional numerical functions (orbitals) are used to construct an antisymmetric many-electron wave function of the restricted open-shell Hartree-Fock model. The orbitals are obtained by solving the Hartree-Fock equations as coupled two-dimensional second-order (elliptic) partial differential equations (PDEs). The Coulomb and exchange potentials are obtained as solutions of the corresponding Poisson equations. The PDEs are discretized by the eighth-order central difference stencil on a two-dimensional single grid and the resulting large and sparse system of linear equations is solved by the (multicolour) successive overrelaxation method ((MC)SOR). The self-consistent-field iterations are interwoven with the (MC)SOR ones and orbital energies and nor-

malization factors are used to monitor the convergence. The accuracy of solutions depends mainly on the grid and the system under consideration which means that within double precision arithmetic one can obtain orbitals and energies having up to 12 significant figures. If more accurate results are needed the quadruple precison floating-point arithmetic can be used.

*Reasons for the new version: additional features, many modifications and corrections, improved convergence rate, overhauled code and documentation**

*Summary of revisions: see ChangeLog found in tgz archive**

Restrictions: The present version of the program is restricted to 60 orbitals. The maximum grid size is determined at compilation time.

Unusual features: The program uses two C routines for allocating and deallocating memory. Several BLAS (Basic Linear Algebra System) routines are emulated by the program. When possible they should be replaced by their library equivalents.

Additional comments: automake and autoconf tools are required to build and compile the program; checked with f77, gfortran and ifort compilers

Running time: Very case dependent – from a few CPU seconds for the H_2 defined on a small grid up to several weeks for the Hartree-Fock-limit calculations for 40-50 electron molecules.

1. INTRODUCTION

The modeling of the electronic structure of atoms and molecules has received a great deal of effort over the last 50 years. Nowadays a significant part of CPU power available to the scientific community is used to understand the physical and chemical behaviour of molecular systems by employing a range and/or a mixture of ab initio, semi-empirical and molecular mechanics methods (see for example [**?**]). In mainstream computational quantum chemistry molecular orbitals are expressed as linear combinations of (atomic) basis functions, which allows to treat systems of any composition and geometry. Since in practice basis sets are usually far from being complete, the

calculated properties suffer from so-called basis set truncation errors that are difficult to assess and control. In order to tackle the problem a number of different sequences or families of basis set functions have been developed to make calculations of various systems and properties feasible and credible. By and large calibration of basis sets is based on atomic data which can be obtained by numerical, i.e. basis-set-free methods. That is why nearly fifty years ago there were already first attempts to solve the Hartree-Fock (HF) problem for molecules by reducing it to one-center cases for which well-established numerical methods had already been known [**?** **?** **?** **?** **?**]. This idea was revitalized many years later by Becke, who proposed solving the Hartree-Fock-Slater equations for a general polyatomic molecule via several separate solutions of the appropriately defined atomic-like problems [**?** **?** **?**]. Recently, Shiozaki and Hirata have extended this approach to the HF equations [**?**].

McCullough was the author of the first not fully algebraic, semi-numerical and successful attempt to solve the (multi-configuration) HF equations for diatomic molecules, the so-called the partial-wave self-consistent-field method (PWSCF) [**?** **?**]. In the case of diatomic molecules one can choose a prolate spheroidal coordinate system whose centres coincide with the nuclei: $\xi = (r_A + r_B)/R_{AB}$, $\eta = (r_A - r_B)/R_{AB}$ and the azimuth angles θ ($0 \leq \theta \leq 2\pi$), where atoms A and B are placed along the z-axis at points $(0, 0, -R_{AB}/2)$ and $(0, 0, +R_{AB}/2)$, and r_A and r_B are the distances of a given point from these atomic centres. The cylindrical symmetry of the diatomic systems allows for factoring out (and later treating analytically) the angular part and expressing molecular orbitals and the corresponding Coulomb and exchange potentials in the form $f(\xi, \eta)e^{im\theta}$ where m is an integer. Thus, for diatomic molecules, the three-dimensional HF equations can be reduced to their two-dimensional counterparts for the functions $f(\xi, \eta)$. In the PWSCF method, these equations are further simplified by requiring that the function f has the form $f(\xi, \eta) = \sum_{l=m}^{l_{max}} X^m(\xi) P_l^m(\eta)$, where the associate Legendre functions $P_l^m(\eta)$ form a basis set in the η variable (that was the reason why McCullough referred to this method as a *semi-numerical* one). As a result, $X^m(\xi)$ functions must satisfy second-order ordinary differential equations which are solved numerically on a properly chosen grid. In the early 1980s, Becke developed a numerical approach for solving density functional equations for diatomic molecules by using polynomial spline interpolation for approximating the f function on a suitable chosen two-dimensional grid [**?** **?** **?** **?**]. The function values at the grid points were obtained by requiring the minimiza-

tion of a certain functional equivalent to the given Fock-Slater equations. Recently, Artemyev et al. proposed a variant of PWSCF by expanding the f function in a finite B-splines basis set; as a bonus one gets also virtual molecular orbitals that can be used to calculate correlation effects by the second-order perturbation theory [**?**]. In the second half of the 1980s Heinemann, Fricke and coworkers showed that the two-dimensional Hartree-Fock equations could be successfully solved by the finite element method [**?** **?** **?**]. Later, a multigrid variant of the method was also developed [**?**]. The finite element approach was also used to solve the one-electron Schrödinger equation for the linear triatomic molecule H_3^{2+} [**?**] and Dirac and Dirac-Slater equations [**?** **?** **?**]. Sundholm and Olsen have also developed a finite element approch for solving the HF equations [**?** **?** **?**]. Recently, Morrison et al. have been advocating the theory of domain decomposition that could be used to divide the variable domain of a diatomic molecule into separate regions in which the HF equations are solved independently by approximating the f function by high-order spline functions [**?** **?**]. Due to this decomposition fast iterative methods can be applied to solve the HF equations in the interior region (where the operators are self-adjoint) and explicit methods in the boundary ones. This scheme allows one to use non-uniform multiple grids and thus solve the HF equations for both bound and continuous eigenstates.

Yet another approach to solving the HF equations for diatomic molecules was put forward in the early 1980s by Laaksonen, Pyykkö and Sundholm. They proposed representing the f function through its values on a two-dimensional mesh. To this end, the second-order partial differential equations for orbitals and potentials were discretized by means of the sixth-order cross-like stencil, and the ensuing large and sparse systems of linear equations were solved by means of the iterative successive overrelaxation (SOR) method [**?**]. This approach will be referred to as the finite difference HF (FD HF) method. Davstad has also developed a fully numerical finite difference approach for the solution of Hartree-Fock equations for diatomic molecules [**?**]. The FD and FE methods together with the wavelets method belong to the so-called real-space mesh techniques used to solve Poisson, Poisson-Boltzmann and eigenvalue problems, and the reader is referred to review articles by Beck [**?**] and Arias [**?**] for further details.

The present author got interested in the FD HF method about 20 years ago and has been involved in its development and applications ever since [**?** **?** **?**]. An improved version of the FD HF method was announced in 1996 [**?** **?**]. For many years the method was mainly used to assist the process of

development and calibration of sequences of universal even-tempered basis sets that was initiated by Moncrieff and Wilson in the early 1990s [**?** **?** **?** **?** **?** **?** **?** **?** **?** **?** **?** **?**]. In the course of that work the method proved to be a reliable source of reference values of total energies, multipole moments, static polarizabilities and hyperpolarizabilities (α_{zz}, β_{zzz}, γ_{zzzz}, $A_{z,zz}$ and $B_{zz,zz}$) for atoms, diatomic molecules and their ions [**?** **?** **?** **?** **?**]. It also provided HF-limit values for examining the convergence patterns of properties calculated using correlation-consistent basis sets within the context of complete basis set models [**?** **?** **?** **?** **?**] and eventually helped in the development of polarization-consistent basis sets [**?** **?** **?**]. The method was also employed to provide the reference values of spectroscopic constants of several diatomic molecules in order to compare the convergence patterns of the correlation-consistent and polarization-consistent basis sets towards the complete basis set limit [**?**]. The FD HF energies accurate to at least 1μHartree were calculated for 27 diatomic transition-metal-containing species in order to investigate the convergence of the HF energies upon increasing the sizes of correlation-consistent basis sets and augmented basis sets developed for the transition atoms by Balabanov and Peterson [**?** **?**]. The correlation-consistent basis sets were not constructed to allow for extrapolation of the HF total energies but rather to extrapolate the correlation energies to the complete basis set limit. It was demonstrated that the correlation energies converge according to the inverse power law while the HF energies exhibit exponential behaviour both with respect to the total number of the basis functions of a given type and with respect to the maximum angular momentum functions included [**?** **?**]. That was the rationale behind Jensen's project to design hierarchies of polarization-consistent basis sets specifically tailored to facilitate extrapolation of the HF (also density functional theory) energies, dipole moments and equilibrium distances to their corresponding complete basis set limits [**?**]. Recently, Zhong *et al.* presented a new family of basis sets, called n-tuple-ζ augmented polarized (n=2-6) basis sets, that converge systematically to the complete basis set limits of both the SCF energy and the correlation energy [**?**]. Jensen examined the dependence of FD HF total energies on the grid size for 42 diatomic species composed of the first and second row elements and reported their energies to better than 1 μHartree accuracy [**?**]. Halkier and Coriani used the FD HF-limit value of the electric quadrupole moment of hydrogen fluoride to estimate the basis set truncation errors when performing state-of-the-art calculations to determine the full configuration interaction basis set limit value of this property

[?]. This work is an apparent demonstration that when accurate post-HF treatment is at stake then the basis set development must guarantee that the HF values are also accurate. Similarly, Pawlowski *et al.* used the FD HF method to obtain the dipole polarizability and the second hyperpolarizability of the Ne atom to estimate basis set errors present in the calculations using the CCS, CC2, CCSD and CC3 coupled cluster models and Dunning's correlation-consistent basis sets cc-pVXZ augmented with diffuse functions [?].

A separate problem is the assessment of relativistic basis functions used for solving the Dirac-Fock equations. Although at present there is no relativistic version of the FD HF method, it seems that the method can be used to indirectly assess the quality of the basis sets used for relativistic calculations. Styszyński studied the influence of the relativistic core-valence correlation effects on total energies, bond lengths and fundamental frequencies for a series of hydrogen halide molecules (HF, HCl, HBr, HI and HAt). In order to assess the quality of basis sets and the dependence of spectroscopic constants on the basis set truncation errors the results of the algebraic non-relativistic HF calculations were compared with the corresponding FD HF ones [? ? ?].

It seems that the development and calibration of the basis sets for the calculation of electron momentum densities also benefited from the FD HF method. It allowed one to find large basis set errors in previous computations of these quantities by means of self-consistent-field wave functions often considered to be of near-Hartree-Fock quality [?]. Calculations of the stopping powers and ranges of energetic ions in matter within the semiempirical approach developed by Ziegler, Biersack and Littmark require the knowledge of interatomic potentials [?]. Nordlund *et al.* [?] studied repulsive potentials for C-C, Si-Si, N-Si and H-Si systems and Pruneda and Artacho [?] extended the analysis to C-C, O-O, Si-Si, Ca-O and Ca-Ca systems by calculating the potentials by means of density functional theory and HF methods (both algebraic and fully numerical). In order to test the quality of the basis sets used to obtain the potentials for Kr-C, Xe-C, Au-C and Pb-C diatomics, especially at small interatomic distances, the FD HF method was also employed [? ?]. Numerical orbitals obtained from the method also proved useful in developing a model of high-harmonic generation from diatomic molecules [?].

The FD HF approach proved useful in the density functional theory context to construct and test various functionals [? ? ? ? ? ? ? ?]. Calcula-

tions for systems with finite-size nuclei employing the Gauss or Fermi nuclear charge distribution models can also be made [**?**]. It is worth noting that if the method is applied to a one-electron system it can be treated as a finite difference solver of the Schrödinger equation for the three-dimensional Coulomb and Krammers-Henneberger potentials (and the like) in the cylindrical coordinates [**?**].

As mentioned above, the universal sequences of even-tempered Gaussian basis functions and polarization-consistent basis functions were developed with the help of numerical results by means of the FD HF approach. This calibration work was a major stimulus for developing the method, improving its accuracy, stability and efficiency and thus enlarging its range of applicability. This paper aims at presenting the current version of the program (version 2.0) so that it can be confidently used and further developed should the need arise. The present version of the program is the first one with the version numer explicitly given, as this should help to maintain the code. This work should be viewed as an update to an earlier paper describing the method and the previous version of the program [**?**]. The current and some in-between versions of the program are available from the project's home page http://www.leiflaaksonen.eu/num2d.html.

The paper is organized as follows. The introduction is followed by a general description of the restricted open-shell Hartree-Fock method for diatomic molecules. In section 3, the discretization of second-order partial differential equations is presented, and the usage of the SOR method for solving large and sparse systems of resulting linear equations is described in some detail as this is the crux of the presented approach. In particular, the SCF/SOR iteration patterns and the accuracy of the approach are discussed. The x2dhf program can be used as a solver of one-electron Schrödinger equation in two variables. Section 4 presents additional one-electron potentials that can be selected. The final section 5 is devoted to the x2dhf program itself, its call tree, data structures and workings of the major routines responsible for the SCF and SOR iterations. In order to help checking, correcting and modifying the program the appendices contain various relevant formulae of DFT energy functionals and potentials, finite nucleus models, multipole moments, etc.

2. GENERAL DESCRIPTION

2.1. The restricted open-shell Hartree-Fock method

For an open-shell, M-electron, diatomic molecular system the Hartree-Fock equations are a set of M one-particle (integro-differential) equations (Fock equations)[**?** **?**]

$$F_a\phi_a = \sum_{a=1}^{M} E_{ab}\phi_b, \quad a = 1, \ldots, M \tag{1}$$

where $\phi_a = \phi_a(x, y, z, \sigma)$ are spin-orbitals forming the Slater determinant

$$\Phi = \frac{1}{\sqrt{M!}} \det |\phi_1(1), \phi_2(2), \ldots, \phi_M(M)|$$

being the approximation to the solution of the Schrödinger equation that minimizes the energy functional

$$\langle\Phi| - \sum_a \frac{1}{2}\nabla_a^2 - \frac{Z_A}{r_{aA}} - \frac{Z_B}{r_{aB}} + \sum_{a<b} \frac{1}{r_{ab}} + \frac{Z_A Z_B}{R}|\Phi\rangle$$

It is assumed that atoms A and B having charges Z_A and Z_B are placed along z-axis at points $(0, 0, -R/2)$ and $(0, 0, +R/2)$ and r_{aA} and r_{aB} are the distances of a given particle from these atomic centres separated by R.

The Fock equations can be put in the form

$$-\frac{1}{2}\nabla^2\phi_a = -\left(-\frac{Z_A}{r_{aA}} - \frac{Z_B}{r_{aB}} + \sum_b \left[V_C^b - V_x^{ab}\right] - E_a\right)\phi_a + \sum_{b\neq a} E_{ab}\phi_b \tag{2}$$

where

$$\nabla^2 V_C^a = -4\pi\phi_a^*\phi_a$$

$$\nabla^2 V_x^{ab} = -4\pi\phi_a^*\phi_b \tag{3}$$

are Poisson equations determining the electron-electron Coulomb and exchange potentials via the single-particle and the pair densities, respectively. The Fock equations are solved by the self-consistent-field (SCF) iterative procedure and therefore the right-hand sides of Eq. (**??**) can be treated during each iteration as already known functions since they are determined by

the orbitals obtained in the previous iteration (and approximate potentials are obtained via integration of Eq. (**??**)). Thus, not only the Coulomb and exchange potentials but also the orbitals can be obtained by solving Poisson-type equations.

Diatomic molecules can be described in the prolate spheroidal coordinate system

$$\begin{array}{ll} \xi = (r_A + r_B)/R & 1 \leq \xi < \infty \\ \eta = (r_A - r_B)/R & -1 \leq \eta \leq 1 \\ \theta \ \text{ azimuth angle} & 0 \leq \theta \leq 2\pi \end{array} \tag{4}$$

where r_A and r_B are the distances of a given point from the atomic centres. The cylindrical symmetry of the diatomic systems allows for factoring out (and later treating analytically) the angular part and expressing the orbitals and the potentials in the form

$$\left.\begin{array}{l} \phi_a \\ V_C^a \\ V_x^{ab} \end{array}\right\} = f(\xi,\eta)e^{im\theta} \tag{5}$$

where the parameter m is equal to 0, ± 1, ± 2, ... The energy expression for the restricted open-shell Hartree-Fock (ROHF) method reads

$$E = \sum_a \langle \phi_a | -\frac{1}{2}\nabla^2 + V_n | \phi_a \rangle \, q_a + \sum_{a,b} \langle \phi_a | \, V_C^b \, | \phi_a \rangle \, U_{ab} - \sum_{a,b} \langle \phi_a | \, V_x^{ab} \, | \phi_b \rangle \, W_{ab} \tag{6}$$

where $V_n = -Z_A/r_{aA} - Z_B/r_{aB}$ is the nuclear potential energy operator. q_a is the occupation number for orbital a and U_{ab} and W_{ab} are the corresponding occupation-number-dependent factors for the Coulomb and exchange energy contributions. In order to allow for a more accurate description of orbitals and potentials in the vicinity of the nuclei, the prolate spheroidal coordinates (η, ξ, θ) are transformed into (ν, μ, θ) variables.

$$\begin{array}{ll} \mu = \ \cosh^{-1}\xi & 0 \leq \mu \leq \infty \\ \nu = \ \cos^{-1}\eta & 0 \leq \nu \leq \pi \end{array} \tag{7}$$

Because of this transformation, ϕ_a is a quadratic function of μ and ν for points in the vicinity of the z-axis ($\mu = 0$ corresponds to the Cartesian coordinates $(0, 0, -R/2 \leq z \leq R/2)$, $\nu = 0$ to $(0, 0, z \geq R/2)$ and $\nu = \pi$ to

$(0, 0, z \leq -R/2))$. In the transformed prolate spheroidal coordinates (ν, μ, θ), the "radial" part of the Laplacian reads

$$\frac{4}{R^2(\xi^2-\eta^2)}\left\{\frac{\partial^2}{\partial\mu^2}+\frac{\xi}{\sqrt{\xi^2-1}}\frac{\partial}{\partial\mu}+\frac{\partial^2}{\partial\nu^2}+\frac{\eta}{\sqrt{1-\eta^2}}\frac{\partial}{\partial\nu}-m_a^2\left(\frac{1}{\xi^2-1}+\frac{1}{1-\eta^2}\right)\right\} \quad (8)$$

In Eq. (**??**), m_a is an integer, and it defines the rotation symmetry of the orbitals. The orbitals with $m_a = 0$ are called σ orbitals; π orbitals have $m_a = \pm 1$, δ orbitals have $m_a = \pm 2$, and orbitals with $m_a = \pm 3$ are called φ orbitals, and so on. Orbitals of higher symmetry than φ are not relevant for ordinary diatomic molecules at the Hartree-Fock level. Orbitals with the same "radial" part and with $m = \pm m_a$ belong to the same shell. Since the m-value for the exchange potentials, V^{ab}, is $|m_a - m_b|$, the largest m-value for the exchange potentials becomes $|2\ m_{a,max}|$, where $m_{a,max}$ is the largest orbital m-value.

Multiplying the Fock equation by $-\frac{R^2}{2}(\xi^2-\eta^2)$ yields the working equation for the orbital relaxation in the transformed prolate spheroidal coordinates.

$$\begin{aligned}
&\left\{\frac{\partial^2}{\partial\mu^2}+\frac{\xi}{\sqrt{\xi^2-1}}\frac{\partial}{\partial\mu}+\frac{\partial^2}{\partial\nu^2}+\frac{\eta}{\sqrt{1-\eta^2}}\frac{\partial}{\partial\nu}\right.\\
&-m_a^2\left(\frac{1}{\xi^2-1}+\frac{1}{1-\eta^2}\right)+R[\xi(Z_1+Z_2)+\eta(Z_2-Z_1)]\\
&\left.-\frac{R}{\xi}(\xi^2-\eta^2)\tilde{V}_C+\frac{R^2}{2}(\xi^2-\eta^2)E_a\right\}f_a(\nu,\mu)\\
&+\frac{R}{\xi}(\xi^2-\eta^2)\left(\tilde{V_x}^a+\frac{R\xi}{2}\sum_{b\neq a}E_{ab}f_b(\nu,\mu)\right)=0 \qquad (9)
\end{aligned}$$

In Eq. (**??**) the modified Coulomb $\tilde{V}_C$ and exchange potentials $\tilde{V}_x^a$ have been introduced.

$$\tilde{V}_C^a = R\xi V_C^a/2 \qquad \tilde{V}_x^{ab} = R\xi V_x^{ab}/2 \quad (10)$$

$$\tilde{V}_C = \sum_a \tilde{V}_C^a \qquad \tilde{V}_x^a = \sum_{b\neq a}\tilde{V}_x^{ab}f_b(\nu,\mu) \quad (11)$$

The working equation for the relaxation of the Coulomb and exchange potentials is analogously obtained from the Poisson equation in the transformed

prolate spheroidal coordinates

$$\left\{\frac{\partial^2}{\partial\mu^2}+\left(\frac{1}{\sqrt{\xi^2-1}}-\frac{2\sqrt{\xi^2-1}}{\xi}\right)\frac{\partial}{\partial\mu}+\frac{\partial^2}{\partial\nu^2}+\frac{\eta}{\sqrt{1-\eta^2}}\frac{\partial}{\partial\nu}\right.$$
$$\left.-(m_a-m_b)^2\left(\frac{1}{\xi^2-1}-\frac{1}{1-\eta^2}\right)-\frac{2}{\xi^2}\right\}\tilde{V}^{ab}$$
$$=-\frac{\pi R^3}{2}\xi(\xi^2-\eta^2)f_a(\nu,\mu)f_b(\nu,\mu) \qquad (12)$$

For Coulomb potentials $a=b$ and the m-dependent term disappears. The diagonal and off-diagonal orbital-energy parameters, E_a and E_{ab}, in Eq. (**??**) are calculated as

$$E_a=\langle\phi_a|-\frac{1}{2}\nabla^2+V_n+\frac{2}{R\xi}(\tilde{V}_C-\tilde{V}_x^a)\,|\phi_a\rangle=\langle\phi_a|\,h_a\,|\phi_a\rangle \qquad (13)$$

$$E_{ab}=\frac{q_b}{q_b+q_a}\left(\langle\phi_b|\,h_a\,|\phi_a\rangle+\langle\phi_a|\,h_b\,|\phi_b\rangle\right) \qquad (14)$$

where q_a and q_b are the occupation numbers of orbitals a and b.

2.2. General boundary conditions

The Cartesian coordinates in terms of (ν,μ,θ) read

$$\begin{aligned} x &= \frac{R}{2}\sinh\mu\ \sin\nu\ \cos\theta \\ y &= \frac{R}{2}\sinh\mu\ \sin\nu\ \sin\theta \\ z &= \frac{R}{2}\cosh\mu\ \cos\nu \end{aligned} \qquad (15)$$

and the radial distances from the nuclei, r_1 and r_2, the distance from the geometrical centre, r, and the Cartesian z coordinate are given by

$$\begin{aligned} r_1 &= \frac{R}{2}(\cosh\mu+\cos\nu)=\frac{R}{2}(\xi+\eta) \\ r_2 &= \frac{R}{2}(\cosh\mu-\cos\nu)=\frac{R}{2}(\xi-\eta) \\ r &= \frac{R}{2}\sqrt{\cosh^2\mu+\cos^2\nu-1}=\frac{R}{2}\sqrt{\xi^2+\eta^2-1} \\ \cos\theta &= z/r=\frac{R}{2}\cosh\mu\ \cos\nu/r=\xi\eta/\sqrt{\xi^2+\eta^2-1} \end{aligned} \qquad (16)$$

Eqs. (**??**) reveal an interesting property of the transformation given by Eq. (**??**). If the sign of μ or ν is reversed then the point (x, y, z) goes over into $(-x, -y, z)$. A rotation by π leaves orbitals with even m unchanged but reverses the sign of orbitals with odd m-values. This means that the orbitals and potentials of σ, δ, ... symmetry are even functions of (μ, ν), and the orbitals and potentials of π, φ, ... symmetry are odd ones. Thus we can write

$$\begin{aligned} f(\nu,\mu) &= (-1)^m f(\nu,-\mu) \\ f(\nu,\mu) &= (-1)^m f(-\nu,\mu) \\ f(\pi+\nu,\mu) &= (-1)^m f(\pi-\nu,\mu) \end{aligned} \tag{17}$$

These symmetry relations can be readily used to set the values of f to zero along $(\nu, 0)$, $(0, \mu)$ and (π, μ) boundary lines for orbitals of π, φ, ... symmetry. In the case of σ, δ, ... orbitals these boundary values are obtained by means of either extrapolation or interpolation if the symmetry of the function is taken into account (see Sec. **??**). For homonuclear molecules the functions must be additionally either symmetric or antisymmetric with respect to the reflection at the molecular centre plane ($\frac{\pi}{2}$,μ). As a result we have symmetric σ_g, π_u, δ_g, φ_u, ... and antisymmetric σ_u, π_g, δ_u, φ_g, ... functions.

2.3. Boundary conditions for orbitals at infinity

At the practical infinity, the asymptotic limit may be used to estimate the values of the orbitals in the last few grid points in μ direction. Consider the second-order differential equation

$$\frac{d^2 y_a}{dr^2} = \left(E_a - \frac{g_1(r)}{r} + \frac{g_2(r)}{r^2} \right) y_a = F_a(r) y_a \tag{18}$$

with $y(0) = 0$ and $y(r) \to 0$ as $r \to \infty$, and E_a is the orbital energy. The asymptotic form of $y_a(r)$ can be written as [**?**]

$$y_a(r) \approx \text{const } F_a(r)^{1/4} \exp\left(- \int_{r_0}^{r} F_a(r')^{1/2} dr' \right) \tag{19}$$

By discretizing and approximating the integral by a rectangular rule, the above equation yields the appropriate expression of the boundary condition for the orbitals at the practical infinity in the form

$$y_a(r_{m+1}) \approx y_a(r_m) \left(\frac{F_a(r_m)}{F_a(r_{m+1})} \right)^{1/4} \exp\left(\sqrt{-F_a(r_m)} (r_{m+1} - r_m) \right) \tag{20}$$

2.4. Boundary conditions for potentials at infinity

The boundary conditions for the potentials $\tilde{V}^{ab}$ at the practical infinity are obtained from the multipole expansion. In particular, we have

$$\tilde{V}_C^a = \frac{R\xi}{2} \sum_{k=0}^{k_{max}} Q_{k,0}^{aa} r^{-k-1} \; P_{k,0}(\cos\theta) \tag{21}$$

where $Q_{k,m}^{ab} = \langle \phi_a | r^k P_{k,m}(\cos\theta) | \phi_b \rangle$ are the multipole moments. Due to the non-vanishing centrifugal term for exchange potentials, the additional factor $[(k-|\Delta m|)!/(k+|\Delta m|)!]$ appears. The multipole expansion for the exchange potentials becomes

$$\tilde{V}_x^{ab} = \frac{R\xi}{2} e^{i\Delta m\theta} \sum_{k=0}^{k_{max}} (-1)^{|\Delta m|} \frac{(k-|\Delta m|)!}{(k+|\Delta m|)!} \frac{1}{r^{k+1}} P_{k|\Delta m|}(\cos\theta) Q_{k,\Delta m}^{ab} \tag{22}$$

where $\Delta m = m_b - m_a$, and $P_{k,\Delta m}$ are the associated Legendre functions.[1]

2.5. Evaluation of one- and two-particle integrals

The volume element in the (ν, μ, θ) coordinates is

$$dxdydz \;\; = \;\; \frac{R^3}{8} \sinh\mu \; \sin\nu \; (\cosh^2\mu - \cos^2\nu) \; d\nu d\mu d\theta \tag{23}$$

The expression for the kinetic energy can be calculated in the (ν, μ, θ) coordinates as

$$\begin{aligned} E_T^a \;\; &= \;\; \int\int\int dxdydz \; \phi_a^* \left(-\frac{1}{2}\nabla^2 \right) \phi_a \\ &= \;\; -\frac{\pi R}{2} \int\int \sqrt{(\xi^2-1)(1-\eta^2)} f_a(\nu,\mu) T(\nu,\mu) f_a(\nu,\mu) d\nu d\mu \end{aligned} \tag{24}$$

where

$$T(\nu,\mu) = \frac{\partial^2}{\partial\mu^2} + \frac{\xi}{\sqrt{\xi^2-1}} \frac{\partial}{\partial\mu} + \frac{\partial^2}{\partial\nu^2} + \frac{\eta}{1-\eta^2} \frac{\partial}{\partial\nu} - m_a^2 \left(\frac{1}{\xi^2-1} + \frac{1}{1-\eta^2} \right) \tag{25}$$

[1] In the x2dhf program, the moment expansion for the boundary condition of the potentials is truncated at k_{max}=8 and $\Delta m \leq 4$.

The nuclear potential energy is analogously evaluated as

$$E_n^a = -\frac{\pi R}{2}\int\int \sqrt{(\xi^2-1)(1-\eta^2)}R\left\{\xi(Z_1+Z_2)+\eta(Z_2-Z_1)\right\}f_a^2 d\nu d\mu \quad (26)$$

The two-electron Coulomb- and exchange-energy contributions to the total energy are obtained as

$$\begin{aligned} E_C^{ab} &= \int\int\int dxdydz\ \phi_a \frac{2}{R\xi}\tilde{V}_C^b\phi_a \\ &= \frac{\pi R^2}{2}\int\int \frac{1}{\xi}\sqrt{(\xi^2-1)(1-\eta^2)}(\xi^2-\eta^2)f_a(\nu,\mu)\tilde{V}_C^b f_a(\nu,\mu)d\nu d\mu \quad (27) \\ E_x^{ab} &= \int\int\int dxdydz\ \phi_a \frac{2}{R\xi}\tilde{V}_x^{ab}\phi_b \\ &= \frac{\pi R^2}{2}\int\int \frac{1}{\xi}\sqrt{(\xi^2-1)(1-\eta^2)}(\xi^2-\eta^2)f_a(\nu,\mu)\tilde{V}_x^{ab} f_b(\nu,\mu)d\nu d\mu \quad (28) \end{aligned}$$

3. METHOD OF SOLUTION

3.1. Solving a Poisson-type equation

We face the problem of solving Eq. (**??**) and Eq. (**??**), i.e. a second-order partial differential equation of the form

$$\left\{A(\nu,\mu)\frac{\partial^2}{\partial\nu^2}+B(\nu,\mu)\frac{\partial}{\partial\nu}+C(\nu,\mu)\frac{\partial^2}{\partial\mu^2}+D(\nu,\mu)\frac{\partial}{\partial\mu}+E(\nu,\mu)\right\}u(\nu,\mu)=F(\nu,\mu) \quad (29)$$

defined on a rectangular domain $[0,\pi]\times[0,\mu_\infty]=[-1,1]\times[1,\xi_\infty]$, where $\xi_\infty = 2r_\infty/R$ with the suitably chosen value of r_∞ defining the practical infinity ($r_A, r_B \le r_\infty$). This value must be large enough to guarantee that the boundary conditions derived from the asymptotic form of these equations can be applied.

Several different methods can be used to solve such a problem. The most popular one is to represent the solution as a linear combination of suitably chosen basis functions and treat the problem algebraically by solving the resulting system of linear equations for expansion coefficients. In the context of the HF method for diatomic molecules, the following alternative three approaches have gained some acceptance: the partial-wave self-consistent-field (PWSCF) method of McCullough [**?** **?**], the finite element (FE) HF method of Fricke, Heinemann and Kolb [**?** **?** **?**] and the finite difference

(FD) HF method of Laaksonen, Sundholm, Pyykkö and the present author [**?** **?**]. Within the latter, approach one chooses a suitable grid and approximates the first and second derivatives by finite differences and solves the resulting system of linear equations by an iterative method [**?**]. In (ν, μ) coordinates, the grid points are distributed uniformly according to

$$\nu_{j+1} = \nu_j + h_\nu, \quad \nu_1 = 0, \quad h_\nu = \pi/(N_\nu - 1), \quad j = 1, 2, ..., N_\nu$$

$$\mu_{i+1} = \mu_i + h_\mu, \quad \mu_1 = 0, \quad h_\mu = \mu_\infty/(N_\mu - 1), \quad i = 1, 2, ..., N_\mu \tag{30}$$

where N_ν and N_μ are the number of mesh points in each variable. This distribution corresponds to a non-uniform distribution of points in the (z, x) plane with higher density in the vicinity of the nuclei, as shown on Fig. **??**. Eq. (**??**) is discretized by the $(r + 1)$-point numerical stencil based on the rth-order Stirling interpolation formula [**?**] (see also Appendix **??**). We have

$$\begin{aligned}
\frac{\partial^2}{\partial \nu^2} u(\nu_i, \mu_j) &= \sum_{k=1}^{r/2} d_k^{(\nu\nu)} \left(u(\nu_{i-k}, \mu_j) + u(\nu_{i+k}, \mu_j) \right) + d_{r/2+1}^{(\nu\nu)} u(\nu_i, \mu_j) \\
\frac{\partial}{\partial \nu} u(\nu_i, \mu_j) &= \sum_{k=1}^{r/2} d_k^{(\nu)} \left(u(\nu_{i-k}, \mu_j) - u(\nu_{i+k}, \mu_j) \right)
\end{aligned} \tag{31}$$

where coefficients $d_k^{(\nu\nu)}$ and $d_k^{(\nu)}$ can readily be derived. We employ the following 9-point central difference formulae for the first and second derivatives of a function $f(x)$

$$\begin{aligned}
f_i' &= \frac{1}{840h} \left(3f_{i-4} - 32f_{i-3} + 168f_{i-2} - 672f_{i-1} \right. \\
&\quad \left. + 672f_{i+1} - 168f_{i+2} + 32f_{i+3} - 3f_{i+4} \right) + O(h^8) \\
f_i'' &= \frac{1}{5040h^2} \left(-9f_{i-4} + 128f_{i-3} - 1008f_{i-2} + 8064f_{i-1} - 14350f_i. \right. \\
&\quad \left. + 8064f_{i+1} - 1008f_{i+2} + 128f_{i+3} - 9f_{i+4} \right) + O(h^8)
\end{aligned} \tag{32}$$

where $f_i = f(x_1 + ih_x)$ and x can be either ν or μ variable. In case of a two-dimensional function Eq. (**??**) and Eq. (**??**) yield 17-point cross-like numerical molecules.

When the discretization of Eq. (**??**) is thus performed it is transformed into a matrix equation

$$\mathbf{Ru} = \mathbf{s} \tag{33}$$

where $\mathbf{u}$ and $\mathbf{s}$ are vectors of length $N_\nu N_\mu$ and $\mathbf{R}$ is a large and sparse square matrix (N_ν and N_μ are typically in the range 100-400). When a 5-point stencil is used to discretize an elliptic equation then the resulting system of linear equations can be readily solved since the relaxation of inner grid points requires only the solution to be known at the boundary. When a higher-order discretization is used then additional boundary values are needed and consequently different numerical stencils (dependent on the discretization order and the distance of the grid points from the boundary) need to be used. This is a rather unwelcome complication because it results in algorithm complications and in a decrease in its efficiency. Therefore the FD HF method utilizes the same 17-point cross-like stencil for all grid points at the expense of additional boundary values that have to be calculated. That is why the boundary values at $u(\nu_i, \mu_{N_\mu+k-1})$, $i = 1, \ldots, N_\nu$, $k = 1, \ldots, 4$ are obtained from the known asymptotic behaviour of orbitals and potentials at the practical infinity r_∞ and Eqs. (**??**) can be used to provide the additional values along the remaining sides of the rectangular region $[\nu_1, \nu_{N_\nu}] \times [\mu_1, \mu_{N_\mu}]$. If the solution u is an odd function it vanishes along the $(0, \mu)$, (π, μ) and $(\nu, 0)$ lines and the corresponding values are set to zero. For an even function the values are calculated using the Lagrange 9-point interpolation formula for an equally spaced abscissas [**?**]

$$f(x_0 + ph) \approx \sum_k A_k^n(p) f_k \tag{34}$$

where A_k^n is the interpolation constant given for even and od velues of n by the following formulae

$$A_k^n(p) = \frac{(-1)^{\frac{1}{2}n+k}}{\left(\frac{n-2}{2}+k\right)!\left(\frac{1}{2}n-k\right)!\,(p-k)} \prod_{t=1}^{n} \left(p + \frac{1}{2}n - t\right), \quad -\frac{1}{2}(n-2) \le k \le \frac{1}{2}n$$

$$A_k^n(p) = \frac{(-1)^{\frac{1}{2}(n-1)+k}}{\left(\frac{n-1}{2}+k\right)!\left(\frac{n-1}{2}-k\right)!\,(p-k)} \prod_{t=0}^{n-1} \left(p + \frac{n-1}{2} - t\right), \quad -\frac{1}{2}(n-1) \le k \le \frac{1}{2}(n-1)$$

Assuming that $f(-x_i) = f(x_i)$ and $f_k = f(x_0 + kh)$ the rearrangement of the expression for f_5 yields

$$f_0 = \frac{1}{126}(210 f_1 - 120 f_2 + 45 f_3 - 10 f_4 + f_5) \tag{35}$$

Hence one can treat all the inner mesh points on an equal footing and perform the discretization of Eq. (**??**) by means of a single pair of numerical stencils as defined by Eqs (**??**).

Since the **R** matrix is large and sparse, an iterative method must rather be used to solve the system of linear equations. In the case of the FD HF method, the orbitals and potentials are solved using the successive overrelaxation method (SOR) and its multicolour variant (MCSOR), which is better suited for vector processors [**?** **?** **?**] (see also sec. **??**, p. **??** and sec. **??**, p. **??**). The standard discretization of Eq. (**??**) by the second-order cross-like stencils and the natural row-wise ordering of grid points (bottom to top, left to right) leads to a tridiagonal matrix with fringes [**?**]. The SOR method can be used to solve such a system and the method is guaranteed to converge if the matrix **R** is symmetric, positive definite and the relaxation factor, ω, is within the interval $0 < \omega < 2$ [**?** **?**]. The $(n+1)$-th iterate of **u** is obtained as

$$R_{pp}u_p^{(n+1)} = (1-\omega)R_{pp}u_p^{(n)} - \omega\left(\sum_{q=1}^{p-1} R_{pq}u_q^{(n+1)} + \sum_{q=p+1}^{N_\nu N_\mu} R_{pq}u_q^{(n)} - s_p\right),\ p = 1,\ldots,N_\nu N_\mu \tag{36}$$

Assuming the natural rowwise ordering of grid points let us write Eq. (**??**) without explicit reference to matrix **R**. Applying the idea of the SOR method to Eq. (**??**) discretized by formulae of Eq. (**??**) we have

$$\begin{aligned} G(\nu_i,\mu_j)u^{(n+1)}(\nu_i,\mu_j) &= (1-\omega)G(\nu_i,\mu_j)u^{(n)}(\nu_i,\mu_j) + \omega F(\nu_i,\mu_j) \\ &\quad -\omega\sum_{k=1}^{r/2}\Big[\ A(\nu_i,\mu_j)d_k^{(\nu\nu)}\left(u^{(n+1)}(\nu_{i-k},\mu_j) + u^{(n)}(\nu_{i+k},\mu_j)\right) \\ &\quad\quad +B(\nu_i,\mu_j)d_k^{(\nu)}\ \left(u^{(n+1)}(\nu_{i-k},\mu_j) + u^{(n)}(\nu_{i+k},\mu_j)\right) \\ &\quad\quad +C(\nu_i,\mu_j)d_k^{(\mu\mu)}(u^{(n+1)}(\nu_i,\mu_{j-k}) + u^{(n)}(\nu_i,\mu_{j+k})) \\ &\quad\quad +D(\nu_i,\mu_j)d_k^{(\mu)}\ \left(u^{(n+1)}(\nu_i,\mu_{j-k}) + u^{(n)}(\nu_i,\mu_{j+k})\right)\Big] \end{aligned}$$

where

$$G(\nu_i,\mu_j) = A(\nu_i,\mu_j)d_{r/2+1}^{(\nu\nu)} + C(\nu_i,\mu_j)d_{r/2+1}^{(\mu\mu)} + E(\nu_i,\mu_j) \tag{37}$$

and $i = 2, \ldots, N_\nu - 1$, $j = 2, \ldots, N_\mu - 1$, i.e. only the interior grid points are relaxed (see also Sec. (**??**), p. **??**).

The convergence of the SOR method depends critically on the value of the overrelaxation parameter ω as shown in Table **??**. For a Poisson equation discretized by the second-order stencil one can show that the optimum value of the overrelaxation parameter ω_{opt} is given by the formula [**?**]

$$\omega_{opt}(N_\nu, N_\mu) = \frac{2}{1 + \sqrt{1 - \rho(N_\nu, N_\mu)^2}} \tag{38}$$

where $\rho(N_\nu, N_\mu)$ is the spectral radius of the corresponding matrix and is equal to $\cos(\pi/N_\nu)/2 + \cos(\pi/N_\mu)/2$. There are no analogous results for higher-order discretizations and for general elliptical second-order partial differential equations like Eq. (**??**) that must be solved to obtain orbitals and potentials of the FD HF method. However, it has been shown that the (near) optimal value of the overrelaxation parameter for orbitals and potentials can be approximated by the formula

$$\omega_{opt}(N_\nu, N_\mu) = \frac{2A}{1 + \sqrt{1 - \rho(N_\nu, N_\mu)^2}} + B \tag{39}$$

where A and B are determined from numerical experiments [**?**]. In order to reliably determine ω_{opt} for, say, orbitals, the potentials must be kept frozen and vice versa. The actual optimal values of the overrelaxation parameters used by the FD HF program are somewhat smaller since usually both orbitals and potentials are relaxed in every SCF iteration, and as a consequence the functions $E(\nu, \mu)$ and $F(\nu, \mu)$ also change.

3.2. Numerical differentiation and integration

Since the differentiation operator in μ and ν directions are independent, the differentiation over these variables can be performed separately. The differential operator in the μ-direction reads

$$D(\mu) f(\nu, \mu) = \left(\frac{\partial^2}{\partial \mu^2} + \frac{\xi}{\sqrt{\xi^2 - 1}} \frac{\partial}{\partial \mu} \right) f(\nu, \mu) = \left(\frac{\partial^2}{\partial \mu^2} + \tilde{\xi}(\mu) \frac{\partial}{\partial \mu} \right) f(\nu, \mu). \tag{40}$$

Let

$$\frac{df}{d\mu}(\nu_i, \mu_j) = \sum_{k=-4}^{4} d_k^{(1\mu)} f(\nu_i, \mu_{j+k}) \tag{41}$$

$$\frac{d^2 f}{d\mu^2}(\nu_i, \mu_j) = \sum_{k=-4}^{4} d_k^{(2\mu)} f(\nu_i, \mu_{j+k}) \tag{42}$$

where $d_k^{(1\mu)}$ and $d_k^{(2\mu)}$ are defined by Eq. (**??**) and Eg. (**??**), respectively. To define $D(\mu_j)f(\nu_i, \mu_j)$ we write

$$\begin{aligned} D(\mu_j)f(\nu_i, \mu_j) &= \sum_{k=-4}^{4} [d_k^{(2\mu)} + \tilde{\xi}(\mu_j) d_k^{(1\mu)}] f(\nu_i, \mu_{j+k}) = \sum_{k=-4}^{4} f(\nu_i, \mu_{j+k}) \tilde{d_k}^{\mu}(\mu_j) \\ &= (\mathbf{f}^{\mu_j} \tilde{\mathbf{d}}^{\mu_j})_i, \qquad \mu_{j+k} = \mu_j + k h_\mu. \end{aligned} \tag{43}$$

where $\mathbf{f}^{\mu_j}$ matrix is (virtually) built from the 9 consecutive columns of $\mathbf{f}$ beginning with the $(j-4)$th column and $\tilde{\mathbf{d}}^{\mu_j}$ is the jth column of the array $\tilde{\mathbf{d}}^{\mu}$, i.e. $(\tilde{\mathbf{d}}^{\mu})_{kj} = \tilde{d_k}^{\mu}(\mu_j)$. Thus evaluation of $D(\mu_j)(\nu_i, \mu_j)$ for all ν values ($i = 1, 2, \ldots, n_\nu$) can be performed via a single matrix times vector multiplication (cf. routine `diffmu`).

The differentiation in ν-direction is performed analogously and the differential operator in the ν-direction reads

$$D(\nu)f(\nu, \mu) = \left(\frac{\partial^2}{\partial \nu^2} + \frac{\eta}{\sqrt{1-\eta^2}} \frac{\partial}{\partial \nu} \right) f(\nu, \mu) = \left(\frac{\partial^2}{\partial \nu^2} + \tilde{\eta}(\nu) \frac{\partial}{\partial \nu} \right) f(\nu, \mu). \tag{44}$$

In the finite difference matrix representation it becomes

$$D(\nu_i)f(\nu_i, \mu_j) = \sum_{k=-4}^{4} f(\nu_{i+k}, \mu_j) \tilde{d_k}^{\nu}(\nu_i) = (\mathbf{f}^{\nu_i} \tilde{\mathbf{d}}^{\nu_i})_j, \qquad \nu_{i+k} = \nu_i + k h_\nu \tag{45}$$

where $\mathbf{f}^{\nu_i}$ matrix is build from the 9 consequitive columns of $\mathbf{f}^T$ (the transposed $\mathbf{f}$ matrix) beginning with the column $i-4$ (cf. routine `diffnu`).

The integrals are evaluated using a two-dimensional generalization of 7-point one-dimensional integration formulae

$$\int_{x_1}^{x_7} dx f(x) = \frac{h}{140}(41 f_1 + 216 f_2 + 27 f_3 + 272 f_4 + 27 f_5 + 216 f_6 + 41 f_7) + O(h^9) \tag{46}$$

The two-dimensional integration weights are obtained as an outer product of the integration weights listed in Eq. (**??**). The order of the integration

formula determines the number of grid points in both directions. In the case of the 7-point integration formula the number of grid points in ν and μ direction has to be of the form $6n + 1$.

The discretized orbitals and potentials can be represented as two-dimensional arrays $\mathbf{f}$ such that $\mathbf{f}_{ij} = f(\nu_i, \mu_j)$, $i = 1, \ldots, N_\nu$, $j = 1, \ldots, N_\mu$, $\nu_i = (i-1)h_\nu$ and $\mu_j = (j-1)h_\mu$. Employing the two-dimensional integration formula that can be derived from Eq. (**??**) one can write

$$\int_0^\pi d\nu \int_0^{\mu_\infty} d\mu J(\nu,\mu) f(\nu,\mu) = \sum_{i=1}^{N_\nu}\sum_{j=1}^{N_\mu} c_i c_j f(\nu_i,\mu_j) J(\nu_i,\mu_j) \quad (47)$$

$$= \sum_{i=1}^{N_\nu}\sum_{j=1}^{N_\mu} \tilde{c}_{ij} f_{ij} = \sum_{k=1}^{N_\nu N_\mu} \tilde{\mathbf{c}}_k \mathbf{f}_k,$$

$$k = (j-1)N_\nu + i \quad (48)$$

where $\tilde{\mathbf{c}}$ is a one-dimensional array of the integration weights merged with the Jacobian and $\mathbf{f}$ is a two-dimensional array of $f(\nu_i, \mu_j)$ values which is treated as a one-dimensional array. Thus the integral can be evaluated as a dot product of the two vectors $\tilde{\mathbf{c}}$ and $\tilde{\mathbf{f}}$ and the integrals defined by Eqs. (**??**), (**??**), (**??**), (**??**) can be dealt with straightforwardly.

3.3. SCF and SOR iteration patterns

The salient feature of the finite difference Hartree-Fock method is the fact that the self-consistent-field iterative process of the Hartree-Fock method and the successive overrelaxation iterations needed to solve the equations are tightly interwoven. A certain number of successive overrelaxation iterations is carried out to update the values of orbitals and potentials between two successive self-consistent-field iterations when the orbital energies are recalculated, the orbitals reorthogonalized and the boundary values at μ_∞ reevaluated (the remaining boundary values are updated at every SOR iteration). Note that, because of the iterative nature of the SOR method, at no single SCF iteration the set of approximate linear equations is solved exactly (and it need not be). Accurate solutions (up to roundoff errors) of the set of the linear equations and thus the Hartree-Fock equations are only obtained when the SCF/SOR process converges (the convergence depends on the electronic configuration of a system, the initial estimates of orbitals and potentials and the parameters used during the SOR iterations).

When performing calculations for an N-orbital atomic or diatomic system a single SCF iteration requires the relaxation of N Fock equations to obtain the orbitals, N Poisson equations for the Coulomb potentials and about $N^2/2$ Poisson equations for the exchange potentials. For example, in the case of the GaF molecule in each SCF iteration one has to relax 2×15 equations for orbitals and Coulomb potentials and 120 equations for the exchange potentials. It has been observed that 65-90% of the CPU time devoted to a given case is spent relaxing orbitals and potentials and that the rate of convergence of the SCF process is mainly determined by the convergence behaviour of these relaxations. That is why the proper choice of the overrelaxation parameters ω_{orb} and ω_{pot} is so important for the efficiency of the FD HF approach. It also effects the patterns of SCF convergence process. Figures (**??**) and (**??**) show the convergence of the individual FH orbitals when some rather suboptimal overrelaxation parameters are used ($\omega_{orb} = 1.65$ and $\omega_{pot} = 1.68$). Initial estimates of the orbitals and potentials are crude and it takes several hundred iterations for the SCF process to settle (about 250 for the 1 σ orbitals and twice as much for the 2 σ one). The convergence is exponential and the rate is nearly constant over the next ten thousand iterations. Only in case of the 2 σ orbital and just after 6000 iterations one can notice a sudden variation in the rate of convergence which lasts for about 500 iterations. It must be kept in mind that in each SCF iteration every orbital and potential undergos by default ten SOR sweeps. It means that at no single SCF iteration we are seeking an exact (within roundoff errors, of course) solutions of the Poisson equations for orbitals and potentials. Instead, due to the iterative nature of the SOR method the solutions are gradually improved.

When a near optimal parameter is used for orbitals and potentials, namely $\omega_{orb} = 1.950$ and $\omega_{pot} = 1.989$, the smoothing out of the convergence pattern takes about 750 SCF iterations but the convergence is six times faster; see Fig. **??** and Fig. **??**. Because of this sort of behaviour it is not recommended to use near optimal values of overrelaxation parameters at the onset of the SCF process when initial estimates of orbitals and potentials are poor as this may easily cause the SCF process to go astray. Instead, one should rather use conservative values for the overrelaxation parameters for a couple of hundred iterations, save the orbitals and potentials and then restart the program with these functions as good initial estimates and the near optimal ω_{orb} and ω_{pot} parameters to speed up the relaxation process. A similar overall convergence pattern can be seen by plotting the total energy differences calculated every tenth SCF iteration, as shown in Fig. **??**.

The number of sweeps that are performed for every single function undergoing relaxation is an adjustable parameter, and it can be set within the range 10-40 without drastically changing the convergence rate. Table **??** shows the dependence of the total number of SOR iterations and the time required to solve the FD HF equations on the number of SOR iterations applied to relax the orbitals and potentials in a single SCF iteration. The problem has not been thoroughly examined but it seems that the optimum value of this parameter cannot easily be found and the net effect may not be worth the effort.

3.4. Accuracy of the method

The FD HF method is a truly basis-set-independent approach and if the mesh and r_∞ are chosen adequately the HF orbitals can be obtained to the required accuracy (within double- or quadruple-precision arithmetic). In order to see this, let us consider the Fock equation for an orbital ϕ (a subscript is omitted for readability) at a given SCF iteration, i.e. we assume that the Fock operator does not depend on its eigenfunctions

$$F\phi = E\phi$$

where

$$\phi = \sum_{i=1}^{\infty} c_i \chi_i$$

is expanded into a complete set of orthonomal basis functions χ_i. When a finite basis set is used an approximate solution is written as

$$\tilde{\phi} = \sum_{i=1}^{M<\infty} \tilde{c}_i \chi_i$$

and the Fock equation is transformed into an approximate one

$$F\tilde{\phi} = \tilde{E}\tilde{\phi}$$

One can write

$$\phi = \tilde{\phi} + \Delta\phi \tag{49}$$

where the truncation error $\Delta\phi$ is orthogonal to $\tilde{\phi}$ or otherwise $\Delta\phi$ would be included in $\tilde{\phi}$. However, $\left\langle \tilde{\phi} \middle| \Delta\phi \right\rangle = 0 + \delta_{\text{roundoff}}$, i.e. the orthogonality

condition is limited by the degree of the linear dependence within a given basis set, which is directly related to accuracy of floating-point arithmetic (δ_{roundoff}). Therefore

$$E = \langle\phi| F |\phi\rangle = \tilde{E} + 2\delta_{\text{roundoff}}\tilde{E} + \langle\Delta\phi| F |\Delta\phi\rangle$$

Usually when an algebraic method is employed to solve the Fock equations the roundoff errors are much smaller than basis set truncation errors. Hence the orbital energies are calculated to a higher accuracy than the orbitals themselves, and that is the reason why the calculations of properties are often regarded as a much more sensitive test of the quality of a given basis than the total energy alone.

When the finite difference solution of the Fock equation is attempted, Eq. (**??**) can still be used but one can no longer assume that $\tilde{\phi}$ and $\Delta\phi$ are orthogonal since now the orbital error is due to both roundoff and discretization errors. When calculations are carried out in double precision arithmetic the former are (usually) much smaller than the latter. The accuracy of the energy can be increased by changing the grid size as long as the discretization errors are larger than the roundoff ones. Thus

$$\left\langle\tilde{\phi}\right| \Delta\phi\Big\rangle = 0 + \delta_{\text{discr}} + \delta_{\text{roundoff}}, \quad \delta_{\text{discr}} \gg \delta_{\text{roundoff}}$$

and the orbital ϕ can only be normalized up to the discretization errors. Therefore

$$E = \langle\phi| F |\phi\rangle = \tilde{E} + 2\delta_{\text{discr}}\tilde{E} + \langle\Delta\phi| F |\Delta\phi\rangle$$

i.e. the orbital energy error depends linearly on the orbital error which, in this case, is mainly due to the discretization. If the changes of the Fock operator during the SCF process were taken into account, the error analysis would be more complicated. However, the linear dependence of the total energy on discretization errors can still be observed, as the data for the hydrogen and helium atoms collected in Tables **??** and **??** show.

The approximate character of the 1 σ orbital can be well monitored by calculating the total electronic dipole moment (along the z-axis) of the system. Clearly, the accuracy of the total energy as measured by the error of the virial ratio closely matches the quality of the orbital. And in this particular case grids larger than $[151 \times 193/25]$ cannot improve the solution of the HF equation.

In order to obtain accurate solutions of the FD HF equations one has to quarantee that both a single orbital and a single Coulomb or exchange

potential are calculated to a high and comparable accuracy. Let us examine solutions of the Fock equations first. Table **??** contains eigenvalues of several σ, π, δ and φ states of the GaF^{+39} system obtained by solving the Fock (Schrödinger) equation by means of the FD method together with the corresponding values obtained from Power's program that generates eigenvalues for the bare-nuclei one-electron diatomic systems [**?**] (Power's program used to be available from Quantum Chemistry Program Exchange, Indiana University). The agreement is perfect, and small discrepancies can be attributed to inevitable roundoff errors.

The overall quality of the FD HF method for diatomics can be examined by applying it to an atomic system that can be described by a single Slater determinant (especially a closed-shell one) since the numerical HF results for atoms are readily available. Table **??** shows the orbital and the total energies of the calcium atom obtained by means of the modified finite difference one-dimensional HF program of Froese Fischer [**?** **?**] and its two-dimensional counterpart (the internuclear separation between the atom and its non-existent partner, i.e. a centre with no charge, was set to 2 au, since such a choice of separation guarantees that similar grids are used when solving the FD HF equations for the atom and the diatomic molecule). This comparison demonstrates that the accuracy of the two methods matches very well. This level of agreement can only be obtained when the one-dimensional grid is large enough and carefully chosen (one has to adjust the ρ_0 and h parameters which determine the first non-zero value of the radial variable and the step size, respectively). Both programs can deliver total energies that have 12-13 significant figures, and it seems that this is the ultimate accuracy that can be expected from finite difference programs that use double-precision arithmetics for floating-point operations. Since the FD HF program treats atomic and diatomic systems on an equal footing, we expect that the same level of accuracy can be obtained when solving the HF equations for diatomic molecules. That this is indeed the case can be seen from Table **??**, where the total HF energies of the beryllium atom and for the LiH, BH and N_2 molecules calculated by means of the FD method and the multigrid finite element method are compared. The highly accurate finite element results correspond to the extrapolated values obtained from a series of calculations performed on grids of increasing density [**?**].

3.5. Efficiency of the method

The analysis of numerical complexity of the three alternative methods of solving the HF equations for diatomic molecules, i.e. PWSCF, FD and FE, show that the FD method is about ten-fold more efficient than the other approaches [**?**]. This is mainly due to the fact that in the FD method the SCF iterations are interwoven with only a small number of SOR relaxation sweeps. This means that in a given SCF iteration the Fock and Poisson equations are not solved exactly by the SOR method but that the solutions are gradually improved and one gets the correct solution only upon the convergence of both the SCF and SOR iterations. Various improvements introduced into the FD HF method in the course of its development have resulted in a considerable increase in its efficiency, and therefore this method can be applied routinely to small- and medium-size diatomic molecules. Of course, as a result of the constant enhancement in computer performance the notion of a medium-size molecule refers to larger and larger systems: a decade ago to systems containig about 10-15 electrons, nowadays to 35-45.

The program allocates memory according to the case under consideration, i.e. the requested number of orbitals and the grid size. This means that the same binary version of the program can be used for systems of variable sizes, or calculation for a given system may be performed with an increasing accuracy.[2] The solutions can be transferred between grids of different densities, which greatly simplifies performing calculations for a series of grids of increasing density.

In the FD HF method the orbital and the potential functions $\mathrm{u}(\nu, \mu)$ are discretized on the rectangular region using meshes with N_ν and N_μ points in the respective variables. The partial differential equations of the HF method in the form of Eq. (**??**) are discretized using the eighth-order central difference expressions, given by Eqs. (**??**) and (**??**), which yield a 17-point cross-like stencil. The use of the 17-point numerical stencil instead of its 13-point counterpart that was employed in the original version of the method [**?**] to discretize the HF equations resulted in the decrease of the truncation errors by two orders of magnitude (from $\mathrm{O}(\mathrm{h}^6)$ down to $\mathrm{O}(\mathrm{h}^8)$). Thus the number of the grid points could be reduced by half without impairing the quality

[2]There are some hard-coded arrays and their dimensions must be adjusted during compilation of the program; see INSTALL file of the x2dhf package.

of the solution.[3] The usage of the higher-order discretization stencil has to be matched with increased accuracy of the numerical integration routines. Therefore, the 5-point (composite) numerical integration was replaced by its 7-point equivalent. The accuracy of the boundary values for the orbitals and potentials at the practical infinity, r_∞, were also increased, which allowed one to decrease this value and reduce the grid size while retaining the overall accuracy. The program was to be used on Cray and Convex computers utilizing vector processors. To make use of this important feature all parts of the program essential for its efficiency were cast in vector-vector, matrix-vector and matrix-matrix form and performed by means of the BLAS library routines. This approach is also advantageous when the program is used on modern superscalar architectures with BLAS library routine support [**?**]. Upon the introduction of these changes it has turned out that the efficiency of the FD HF method depends solely on the efficacy of the method used to solve the systems of linear equations. That is why some effort has been put into the careful implementation of the SOR method (and its multicolour variant) [**?**]. With the 17-point numerical stencil the relaxation of a single grid value requires 56 floating point operations and the process can be performed with speeds of about 1 and 2 GFLOPS for AMD Opteron 2200 (2.8 GHz) and Intel E8400 (3 GHz) processors, respectively.

4. ONE-ELECTRON POTENTIALS

The primary application of the FD HF method is of course solving the Fock equations for diatomic molecules. However, with some modifications it can also be used to solve these sorts of two-dimensional partial differential equations with other one- and two-particle attractive potentials.

4.1. DFT potentials

In particular, the FD HF method can be used to solve the Fock equations with various density functional potentials. The program supports the LDA and B88 [**?**] local exchange potentials and the LYP [**?**] and VWN [**?**] correlation potentials; the corresponding formulae for potentials and energies together with the relevant references can be found in Appendix **??**, p. **??**. Table **??** presents a comparison of total energies of the He, Be and Ne

[3] In case one solves a model Poisson equation the savings due to the higher-order discretization can be even larger.

atoms calculated within the finite basis set and finite difference approaches with various combinations of local exchange (LDA and B88) and correlation potentials (LYP and VWN). The present version of the FD HF program can be used to perform calculations by means of the self-consistent multiplicative constant method of Karasiev and Ludeña [**?**] where the $X\alpha$ exchange potential is used with the α parameter adjusted in every SCF iteration (see Table **??**, **??**). The program also allows one to calculate LDA, B88, PW86, PW91, LYP and VWN contributions to the total energy for any set of orbitals. It is worth mentioning that automatically adjusted values of the relaxation parameters ω_{orb} and ω_{pot} should be avoided when using the local exchange potentials. In such instances one should set these parameters to (sometimes much) smaller values in order to guarantee the convergence of the SCF/SOR process.

The LDA ($X\alpha$) approximation is often used as a handy way of generating good initial estimates of orbitals. In such a case the recommended α values for elements from helium to niobium are taken from Schwarz [**?**] and are extrapolated for the remaining ones. To this end, one can also use the model potential of Green, Sellin and Zachor [**?**]. For a given atom, this potential produces HF-like orbitals, and it was found useful in finding decent starting orbitals for any molecular system.

4.2. Krammers-Henneberger potential

The FD HF program can also be employed to solve the Schrödinger equation for a one-electron diatomic system with an arbitrary but binding potential and it can be treated as a finite difference solver of the Schrödinger equation for the three-dimensional potential in cylindrical coordinates [**?**]. The present version of the program supports the (smoothed) Coulomb potential

$$V = \frac{-V_0}{\sqrt{a^2 + r^2}} = \frac{-V_0}{\sqrt{a^2 + x^2 + y^2 + z^2}}$$

and the Krammers-Henneberger potential

$$V = \frac{-V_0}{\frac{2\pi}{\omega}\sqrt{a^2 + b_x^2 + y^2 + z^2}}$$

with $b_x = x + \alpha_0 + \alpha_0(\cos(\omega t) - 1)$, $\alpha_0 = E_0/\omega^2$, and where a is a width of the model potential, V_0 its depth, E_0 the laser field intensity and ω its cycle frequency.

4.3. Finite field approximation

For diatomic molecules, the z-components of polarizabilities and hyperpolarizabilities can be evaluated by the finite field approximation when the field is applied along the internuclear axis. The effect of this field is attributed by adding terms of the form

$$-\sum_i \mu_z^i(0) F_z \tag{50}$$

to the Hamiltonian where $\mu_z^i(0)$ is the z-component of the permanent dipole moment for the i-th electron. The induced dipole and quadrupole moments can be written as the expansions [**?** **?**]

$$\begin{aligned} \mu_z(F_z) &= \mu_z(0) + \alpha_{zz}F_z + \frac{1}{2}\beta_{zzz}F_z^2 + \frac{1}{6}\gamma_{zzzz}F_z^3 + \cdots \\ \Theta_{zz}(F_z) &= \Theta_{zz}(0) + A_{z,zz}F_z + \frac{1}{2}B_{zz,zz}F_z^2 + \cdots \end{aligned} \tag{51}$$

When the moments are evaluated for 0, $\pm F_z^0$ and $\pm 2F_z^0$ values of the field, the 5-point central difference approximations to the derivatives can be employed, resulting in the following approximate formulae for the dipole polarizability (α_{zz}), and the first and second dipole hyperpolarizabilities (β_{zzz} and γ_{zzzz}), the dipole-quadrupole polarizability ($A_{z,zz}$) and the dipole-dipole-quadrupole hyperpolarizability ($B_{zz,zz}$), respectively

$$\begin{aligned} \alpha_{zz} = \left(\frac{d\mu_z}{dF_z}\right)_{F_z=0} &\approx \frac{\mu_z(-2F_z^0) - 8\mu_z(-F_z^0) + 8\mu_z(+F_z^0) - \mu_z(+2F_z^0)}{12F_z^0} \\ \beta_{zzz} = \left(\frac{d^2\mu_z}{dF_z^2}\right)_{F_z=0} &\approx \frac{-\mu_z(-2F_z^0) + 16\mu_z(-F_z^0) - 30\mu_z(0) + 16\mu_z(+F_z^0) - \mu_z(+2F_z^0)}{12(F_z^0)^2} \\ \gamma_{zzzz} = \left(\frac{d^3\mu_z}{dF_z^3}\right)_{F_z=0} &\approx \frac{-\mu_z(-2F_z^0) + 2\mu_z(-F_z^0) - 2\mu_z(+F_z^0) + \mu_z(+2F_z^0)}{2(F_z^0)^3} \\ A_{z,zz} = \left(\frac{d\Theta_{zz}}{dF_z}\right)_{F_z=0} &\approx \frac{\Theta_{zz}(-2F_z^0) - 8\Theta_{zz}(-F_z^0) + 8\Theta_{zz}(+F_z^0) - \Theta_{zz}(+2F_z^0)}{12F_z^0} \\ B_{zz,zz} = \left(\frac{d^2\Theta_{zz}}{dF_z^2}\right)_{F_z=0} &\approx \frac{-\Theta_{zz}(-2F_z^0) + 16\Theta_{zz}(-F_z^0) - 30\Theta_{zz}(0) + 16\Theta_{zz}(+F_z^0) - \Theta_{zz}(+2F_z^0)}{12(F_z^0)^2} \end{aligned} \tag{52}$$

In principle, the polarizability and the first hyperpolarizability can also be evaluated as the second and the third derivatives of the total energy with

respect to the field, i.e.

$$\alpha_{zz} = -\left(\frac{d^2E}{dF_z^2}\right)_{F_z=0} \qquad \beta_{zzz} = -\left(\frac{d^3E}{dF_z^3}\right)_{F_z=0} \tag{53}$$

and approximated by the above finite differences accordingly. However, this approach is less preferable, as it requires total energy values of very high quality to be applied in a numerically stable fashion. The calculations of (hyper)polarizabilities by means of Eqs (**??**) seems to be a straightforward procedure but it also requires very accurate values of the dipole moment, especially when the second dipole hyperpolarizability values are of interest. This is readily seen from Table **??**, where the values of the total energies and the dipole and quadrupole moments of hydrogen fluoride obtained for five different values of the electric field are examined. The upper part of the table contains raw data extracted from the program's listings by a Perl script.[4] This script uses Eqs (**??**) to evaluate the polarizabilities and hyperpolarizabilities from the supplied data. A careful examination of the SCF/SOR iteration process shows that the total energies and multipole moments are known with a relative error of the order 10^{-12}. This information can also be supplied to the script, and the dependence of the electric properties on the quality of the solution estimated. It is worth noting that even the dipole moment calculated by taking the first derivative of the energy has at most four correct figures, and as a consequence leads to the polarizability with only two significant figures. The value of the first hyperpolarizability is completely useless. By contrast, the dipole moment calculated from orbitals inherits their accuracy, and even the second hyperpolarizability can be quoted with 3-4 figures.

The problems with the finite field approach are twofold. First, if the FD HF equations with the Hamiltonian modified by the presence of the external field are solved, the chosen field strength must be small enough to yield converged and numerically stable results. The presence of the external electric field makes it more difficult to apply boundary conditions at infinity. In fact, much larger values of the practical infinity (up to 150-200 bohr) must be chosen in order to converge the SCF/SOR process to high accuracy. As a result, the number of grid points required is increased, thereby raising

[4]The listings and the script can be found in examples/fh and utils subdirectories of the x2dhf package, respectively.

the computational demands of the FD HF calculations, which are already multiplied by a factor of 5 because of the 5-point difference formulae used to calculate the (hyper)polarizabilities. Second, the field must be strong enough to facilitate meaningful numerical differentiation of the dipole moment values for different field strengths. Since it may be difficult to satisfy both requirements, the FD HF equations are usually solved on a number of different grids and with several field strengths.

Recently, this approach has been used to calculate accurate values of polarizabilities and hyperpolarizabilities for atoms, heteronuclear and homonuclear diatomic molecules and their ions [**?** **?**]. The dependence of these properties on the internuclear separation can also be studied, as Table **??** shows. Calculations for atoms and heteronuclear molecules are rather straightforward once the grid is chosen. However, homonuclear systems pose a problem since a weak external electric field breaks the inversion symmetry, and the SCF/SOR iteration process fails to deliver well-converged solutions. It has recently been shown that the problem encountered is due to a near degeneracy of some of the orbitals and this can be circumvented by allowing for non-zero off-diagonal Lagrange multipliers between such orbitals. The modified FD HF method was used to perform calculations of electrical properties for the H_2, Li_2, F_2, N_2 and O_2 molecules and the results can be found in [**?**]. The quality of the properties can be assessed by the examination of the results for the N_2 molecule shown in Table **??**. The values of the polarizability and the first hyperpolarizability should be compared with the best algebraic HF values obtained to date by Maroulis, namely 15.0289 and 799 [**?**].

4.4. Finite nuclei

The FD HF program is also suited to study atomic and diatomic systems with finite nuclei. The charge distribution within a nucleus can be described by either Gaussian and Fermi models [**?**], where parameters defining the atomic masses of the nuclei are taken from the table of atomic masses compiled by Wapstra and Audi [**?** **?**] (see Appendix **??**, p. **??**, for details).

5. DESCRIPTION OF THE CODE

5.1. Structure of the code

It is assumed that the reader has unpacked the program's package and has access to the User's Guide pdf file that can be found in docs directory.

The large scale structure of the program is presented in Fig. **??**.[5] The main routine x2dhf is shown calling the twelve first level routines in the order given, i.e. printBanner is invoked before setPrecision, setDefaults and so forth. The routines of the second and third levels are also given and if their calling order is irrelevant they are put into a box. The program starts by printing its name and version. Then it determines the lengths of integer and floating-point constants and variables since the program can be compiled to support calculations using three different combinations of integer/real data types: i32 (4-byte integers, 8-byte reals), i64 (8-byte integers, 8-byte reals) and r128 (8-byte integers, 16-byte reals); see src/Makefile for details. These values are used for seamless retrieval of binary data when reading orbitals and potentials from disk files. In some cases, especially when quadruple precison calculations are attempted, this is not enough because of non-standard data formats employed by Fortran compilers. In such cases it is recommended to export and import data in formatted instead of unformatted form (see `inout` label). Next the default values of various scalar and array variables are set and the program is ready to read input data. The retrieval of input data is controlled by `inputData` routine and `inCard` routine is used to read a single line at a time and scan it in search for nonspace fields (if an exclamation mark or a hash is found then whatever follows is treated as a comment). Subsequently `inStr`, `inInt` and `inFloat` routines are used to extract string, integer and floating-point data, respectively. The input must contain at least the following cards: TITLE, NUCLEI, GRID, CONFIG, ORBPOT and STOP. TITLE gives at most 80 character-long description of a given case and is used as a label of disk files with orbitals and potentials. NUCLEI card defines the charges of atoms A and B and their separation (in atomic units or angstroms). The grid is specified by providing at least the number of points in the ν variable (N_ν) and the practical infinity (r_∞). The number of point in the μ variable (N_μ) is then subsequently calculated so that the step sizes in both the variables are approximately the same to guarantee a comparable level of truncation errors when performing differentiation and integration of functions. Additionally, N_ν and N_μ are adjusted to the form $6k + 1$ since the numerical integration is based on a 7-point integration formula. If the multicolour SOR method is used then N_ν must be further restricted to the

[5]The x2dhf package contains the file ftnchek_html/CallTree.html which can be used to browse the complete call tree of the program.

form $5k + 6$ in order to subdivide the mesh points into five independent subsets.

The program uses fixed-size common blocks and variable-length arrays to move data between routines. However, the size of some common block arrays is determined during the compilation through MAXNU and MAXMU variables (see src/Makefile.am). These variables set the maximum number of grid points in ν and μ variables, respectively, that can be used when specifying the grid size for a given case. The size of the variable-lenghth arrays is however case dependent and the C routine `memAlloc` is used to allocate the required space. Now `initArrays` is called to perform initialization of various common block variables and common block and variable-length arrays. First of all the subroutine `initCBlocks` initializes grid, orbital and SOR data. Then `initAddr` is called to calculate dimensions of variable-length arrays cw_orb, cw_coul, cw_exch for holding orbitals, Coulomb and exchange potentials and to calculate their respective addresses within these arrays. cw_suppl array is also partitioned and the routine `initSuppl` is called to initialize arrays for one-electron potentials, integration weights and Jacobians for one- and two-particle integrations, etc. `initMesh` is responsible for establishing an order of mesh points. By default the 'middle' type of ordering is chosen but the natural column-wise, row-wise and the reverse natural column-wise orderings can also be selected (see below). Finally `initExWeights` calculates the weights of exchange contributions to the (restricted) open-shell Hartree-Fock energy expression. Now, when the input data are processed the relevant information about the way the given case will be handled can be printed (`printCase`). One can thus check the method that will be applied, the electronic configuration defined and the grid, SCF and SOR parameters. The detected machine accuracy, the values of the π constant and the bohr to angstrom conversion factor together with the summary of memory usage are also printed.

Before the SCF process can begin the initial values of orbitals and Coulomb and exchange potentials must be provided. The molecular orbitals can be formed as a linear combination of either atom-centred hydrogen-like orbitals (via LCAO label, see `initHyd`) or numerical orbitals taken from the atomic HF program (see `initHF`). Good estimates of the molecular orbitals can be obtained by means of the GAUSSIAN package when its appropriate output files are provided (see mkgauss option of `tests/xhf` script). The Coulomb potentials are calculated using the Thomas-Fermi model and the exchange ones are approximated by 1/r (see `initPot`). Unless the LCAO cards are present the contributions from both the centres are taken with equal weights

(in case one of the centres has zero nuclear charge the corresponding mixing coefficient is also set to zero). Of course orbitals and potentials (together with other relevant data) can be retrieved from disk files so that the current case can be treated as a continuation of a previous run of the program.

Now, the initial orbitals can be normalized and orthogonalized and the evaluation of diagonal and off-diagonal Lagrange multipliers can follow (see `prepSCF`). The multiple moments and the total energy are also calculated and the program proceeds to its core `doSCF` routine (see Fig. **??**). There the already calculated multipole moments are used to determine boundary values of Coulomb and exchange potentials at the practical infinity, r_∞ (see `potAsympt`), and the solution of the Poisson equations for potentials can be advanced by perfoming several (10 by default) iterations of the SOR method (see `coulSOR` and `exchSOR`). This is done in the orbital loop for each orbital in turn with the order determined by the electronic configuration as specified by input data, i.e. σ-type orbitals first, then π, δ and φ. For each orbital the updated Coulomb and exchange potentials are used to construct the Fock equation, the boundary values of the orbital at r_∞ are evaluated and the orbital values at the mesh points are updated by performing several SOR iterations (see the discussion of `orbSOR` routine below). Then the orbital is normalized and orthogonalized and the diagonal and, if needed, off-diagonal Lagrange multiplies are recalculated. When all the orbitals are thus processed the convergence criteria are examined. If the SCF iteration limit is reached or the maximum changes of orbital energies and/or their norms meet their respective thresholds the SCF/SOR iteration process terminates. Otherwise the next SCF iteration begins with the recalculation of the multipole moments, if the changes in orbital energies between two consecutive SCF iterations are large enough.

A few more words are needed to clarify the algorithm used to perform SOR iterations. Since the boundary values for the potentials are calculated before calling the `coulSOR` and `exchSOR` routines these are only responsible for relaxing the function values. In Fig. **??** the unnumbered star-like points represent these boundary values. In order to be able to use the same 17-point cross-like stencil for the discretization of the Poisson equation for all (numbered) grid points the function being relaxed is immersed in a larger grid. When the routine `putin` transfers this function from the original grid into its extended counterpart it also sets the values at the bullit-like points using the even or odd symmetry of the function. Now the relaxation can proceed in a chosen given order of grid points (the column-wise in our example). When

the process is over the symmetry of the function can be used again to fix the values of $\times$- and $\otimes$-like grid points: for functions of even symmetry these values are obtained from interpolation or set to zero otherwise (see `sor` routine). The relaxation sweeps (together with the interpolation) are repeated as many times as required and `putout` routine is used to transfter updated function values from the extended grid to the original one. In the case of `orbSOR` routine the local and non-local parts of the Hartree-Fock potential has to be calculated first by calling `fock` routine (see Fig. **??**). Then the asymptotic behaviour of the Fock equation is used to determine parameters needed to calculate the boundary values of orbitals at μ_∞ (see `orbAsymptDet` and `orbAsymptSet`).

Fig. **??** shows the column-wise ordering of mesh points. By default however, the x2dhf program uses the so-called middle-type ordering which results in a bit faster convergence of the SCF/SOR process. As shown in Fig. **??** the μ coordinates change according to the following order $\mu_{(M-1)/2}$, $\mu_{(M-1)/2-1}$, $\ldots$, μ_1, $\mu_{M/2}$, $\mu_{M/2+1}$, $\ldots$, μ_M. For each μ_i the ν coordinates form the sequence: $\nu_{(N-1)/2}$, $\nu_{(N-1)/2-1}$, $\ldots$, ν_1, $\nu_{N/2}$, $\nu_{N/2+1}$, $\ldots$, ν_N, where M and N are number of grid points in each direction undergoing relaxation.

In case the multi-colour SOR is used all the mesh points undergoing relaxation can be subdivided into five colours or colour suits as shown in Fig. **??** (the triangles denote the no trump). It can easily be seen that when the 17-point stencil is used for descritization the relaxation of, say, the clubs points depend only on the values of points of remaining colours. That is why the points of the same colour can be relaxed simultaneously and the algorithm can be vectorized resulting in a five-fold speedups. It is possible to parallelize the method within the OpenMP scheme but unfortunately no gain in efficiency could be obtained. It is hoped that the MCSOR algorithm can be effectively implemented on general-purpose graphics processing units using CUDA technology (http://www.nvidia.com/object/cuda_home_new.html).

In order to help to understand how the program works, a short description of all its most important routines follows in lexicographic order.

`inCard` reads (and echoes) a single line of input data and scans it in search for nonspace fields. If an exclamation mark or a hash is found then whatever follows is treated as a comment. `inStr`, `inInt` and `inFloat` routines are used to extract string, integer and floating-point data, respectively.

`coulAsympt` determines for a given orbital asymptotic values of the corresponding Coulomb potential

`coulMCSOR` prepares the right-hand side of the Poisson equation for a given Coulomb potential and performs the default number of MCSOR iterations (cf. `mcsor`).

`coulMoments` determines the multipole expansion coefficients for Coulomb potentials

`coulSOR` prepares the right-hand side of the Poisson equation for a given Coulomb potential and performs default number of SOR iterations (cf. `sor`). In order to be able to use the same numerical stencil for all grid points `putin` and `putout` routines are used transfer the function between the primary and extended grids.

`doSCF` controls the SCF process. In every SCF iteration orbitals are relaxed in the reverse order as defined by the input data. For a given orbital the boundary values of the corresponding Coulomb and exchange potentials at r_∞ are calculated and the functions are relaxed by performing several SOR iterations. Then the boundary values of the orbital are evaluated and the orbital undergoes SOR relaxations. Next, it is normalized and orthogonalized by means of the Schmidt algorithm. If required, the inversion symmetry of the orbital can also be imposed. Subsequently, its orbital energy and, if necessary, off-diagonal Lagrange multipliers are calculated. This same procedure is repeated for every (non-frozen) orbital. From time to time the `mpoleMom` routine is called and the multipole moments needed to evaluate asymptotic values of potentials are recalculated. Also every declared number of SCF iterations the total energy is calculated and the orbitals and potentials are written to disk. The SCF process is terminated if the convergence criteria are met or the maximum number of SCF iterations is reached.

`Ea` computes the eigenvalue of the Fock equation for a given normalized orbital as

$$E_a =< \phi_a| - \tfrac{1}{2}\nabla^2 + V_n + V_C - V_x^a|\phi_a >.$$

`Eab` computes the off-diagonal Lagrange multiplier for a pair of normalized orbitals.

`EaDFT` computes the eigenvalue of the Fock equation for a given orbital when a local exchange approximation is used.

`EabDFT` computes the off-diagonal Lagrange multiplier for a pair of normalized orbitals in case a local exchange approximation is used.

`Etotal` evaluates the HF total energy.

`EtotalDFT` evaluates the total energy for a given DFT potential.

`exchAsympt` determines from the multipole expansion asymptotic (boundary) values of the exchange potentials entering a given Fock equation.

`exchMCSOR` prepares the right-hand side of the Poisson equation for a given exchange potential and performs the default number of MCSOR iterations.

`exchMom` determines the multipole expansion coefficients for exchange potentials.

`exchSOR` prepares the right-hand side of the Poisson equation for a given exchange potential and performs the default number of SOR iterations.

`initArrays` initializes various common blocks and variable-length arrays.

`initAddr` calculates dimensions of arrays and addresses of particular orbitals, Coulomb and exchange potentials within dynamically allocated arrays cw_orb, cw_coul, cw_exch; arrays cw_suppl and cw_sctch are also partitioned.

`initCBlocks` checks and adjusts the requested dimensions of the grid and initializes some common block arrays with grid, orbital and SOR data.

`initDisk` controls retrieving of orbitals and potentials together with some other data (Lagrange multipliers, multipole moment expansion coefficients, etc.) from disk files in binary or ascii format.

`initExWeights` calculates the weights of exchange contributions to the (restricted) open-shell Hartree-Fock energy expression.

`initGauss` initializes molecular orbitals through the discretization of GAUSSIAN orbitals reconstructed from the GAUSSIAN output (see `prepGauss` for details); Coulomb and exchange potentials are initialized as in `initHyd`.

`initHF` initializes molecular orbitals as a linear combinations of Hartree-Fock orbitals on centres A and B (orbitals are generated by the qrhf program[6]); Coulomb and exchange potentials are initialized as in `initHyd`.

`initHyd` initializes molecular orbitals as a linear combinations of hydrogenic functions on centres A and B; Coulomb and exchange potentials are initialized by calling `initPot`.

`initMesh` establishes ordering of mesh points (cf. `order` label).

`initOrbPot` initializes orbitals and potentials (see `initHyd`, `initHF`, `prepGauss`, `initGauss`, `initDisk` and `initTF` for details).

`initPot` initializes Coulomb potentials as a linear combination of the Thomas-Fermi potentials at the atomic centres. In case of HF calculations exchange potentials are approximated as the corresponding linear combination of 1/r terms. In case of DFT calculations the local exchange approximation is used.

`initSuppl` initializes various supplementary arrays of case-dependent lengths supported by cw_suppl (one-electron potentials, Jacobians, integration weights, etc.).

`inFloat` – see `inCard`.

`inInt` – see `inCard`.

`inputData` handles the input to the x2dhf program.

`inStr` – see `inCard`.

`mcsor` performs one iteration of the multicolour successive overrelaxation scheme.

[6]This is a modified version of Fischer's MCHF program that can be downloaded from http://fizyka.umk.pl/~jkob/qrhf.

`memAlloc` dynamically allocates memory acccording to grid requirements and orbital configuration of the current case (a C routine).

`memDealloc` releases memory allocated by `memAlloc` (a C routine).

`mpoleMom` determines the coefficients of the multipole expansion for Coulomb and exchange potentials (see `coulMom` and `exchMom`).

`norm` performs normalization of a given orbital.

`ortho` performs the Schmidt orthonormalization of a given orbital.

`orbAsymptDet` initializes an array which is used by `orbAsymptSet` to calculate boundary values of a given orbital at practical infinity.

`orbAsymptSet` recalculates asymptotic values of a given orbital at the practical infinity using exponential decay values prepared by calling `orbAsymptDet`.

`orbMCSOR` performs the same tasks as `orbSOR` but uses the MCSOR method for solving the Poisson equation (cf. `mcsor`).

`orbSOR` evaluates the Fock potential (cf. `fock` and `fockDFT`) for a given orbital, sets up the right-hand side of the Poisson equation for that orbital and performs a default number of SOR iterations (cf. `sor`). In order to be able to use the same numerical stencil for all grid points `putin` and `putout` routines are used to transfer functions between the primary and extended grids. `orbAsymptDet` and `orbAsymptSet` are used to calculate boundary values.

`potAsympt` determines from the multipole expansion asymptotic (boundary) values of the Coulomb and exchange potentials needed for a given Fock equation.

`prepGauss` extracts basis set parameters from an output of the GAUSSIAN94/98 program (gaussian.out and gaussian.pun files) to be used by initGauss routine.

`prepSCF` prepares the SCF process by orthogonalizing orbitals, calculation of orbital energies, evaluation of Lagrange multipliers and multipole moment expansion coefficients.

`printBanner` prints the name and version of the program.

`printCase` outputs the information about the case being defined by the input data (molecular system, internuclear separation, configuration, grid, memory requirements, etc.).

`printResults` outputs the results of calculations, i.e. the final total energy together with its contributions, DFT values of Coulomb, exchange and correlation energies, orbital energies and normalization errors, multipole moments and CPU usage.

`putin` takes a function defined on the primary grid and immerses it into the extended grid so that the same 17-point cross-like stencil can be used for the discretization of the Poisson equation for all grid points undergoing relaxation; the odd or even symmetry of the function is used to supply extra boundary values.

`putout` reverses the work of the `putin` routine and transfers a given function values from the extended to primary grid.

`setCi` determines inversion symmetry of a given orbital (or set of orbitals) and sets its value at (ν, μ), where $\nu = \pi/2, \ldots, \pi$ and $\mu = 1, \ldots, \mu_\infty$ by the corresponding values at $\nu = 0, \ldots, \pi/2$.

`setDefaults` sets default values of various scalar and array variables, in particular those responsible for the ordering of mesh points and controlling the SOR relaxations and the SCF process.

`setPrecision` calculates floating-point precision and the lengths of integer and real variables in order to handle input and output data and printouts correctly. On x86 systems the precision depends on compiler optimization flags used and therefore this routine must be compiled with the minimum optimization in order to avoid reporting precision of the extended IEEE 754 arithmetic (see src/Makefile.am).

`sor` performs one iteration of the successive overrelaxation scheme.

`writeDisk` writes molecular orbitals, Coulomb and exchange potentials together with some other data such as Lagrange multiplies, multipole moment expansion coefficients etc. in binary format to disk files.

5.2. Language, features and limitations of the program

Except for two C routines used to allocate and deallocate memory, the program has been written in Fortran 77. Fortran 95 can also be used to compile the program, but no specific features of this version of the language are used. The program uses the `date_and_time` library routine for retrieving from the system the current time and date (see `getDateTime`). To monitor the CPU time spent by the program calculating multipole moments, relaxing orbitals and potentials, etc., the `cpu_time` library routine is used (see `getCpuTime`). Several BLAS routines are emulated by the program. If possible they should be replaced by their optimized equivalents (see INSTALL). The present version of the program is restricted to 60 orbitals. The maximum grid size that can be used is dependent on the case being considered and available memory, and can be modified by the parameters MAXNU and MAXMU (see src/Makefile.am). The maximum number of basis functions used to prepare the initial estimates of orbitals by means of the Gaussian program is restricted in a similar fashion by the parameter MAXBASIS.

The command and data file structure is described in User's Guide, where examples of sample input data cards are also included (see docs/users-guide.-pdf). The latest release of the program together with its description, User's Guide, several examples of its inputs and outputs is available at http://-www.leiflaaksonen.eu/num2d.html.

ACKNOWLEDGEMENTS

My sincere thanks and gratitude are due to D. Moncrieff and S.Wilson for many years of collaborative efforts and their perseverance in making the algebraic and numerical Hartree-Fock results match. I would like to thank I. Grant and F. A. Parpia for allowing me to include in the x2dhf code a routine taken from their GRASP package for calculating the Fermi nucleus potential and J.Karwowski and J.Wasilewski for their interest in the project and many valuable discussions.

Appendix A. DFT exchange and correlation potentials

Appendix A.1. LDA exchange potential

The local density approximation (Xα) potential is defined as

$$V_X(\alpha) = -\frac{3}{2}\alpha\left(\frac{3}{\pi}\right)^{1/3} 2^{-2/3}\sum_{\sigma}\rho_{\sigma}^{1/3} \tag{A.1}$$

In case $\alpha = 2/3$ we have so-called the Slater exchange potential. The corresponding total energy reads

$$E_X(\alpha) = -\frac{9}{8}\alpha\left(\frac{3}{\pi}\right)^{1/3} 2^{1/3}\sum_\sigma \int \rho_\sigma^{4/3} d^3\mathbf{r} \tag{A.2}$$

Appendix A.2. B88 exchange potential

Becke [**?**] proposed the following form of the exchange energy

$$\begin{aligned} E_{B88} &= E_X(2/3) - \sum_\sigma \int \rho_\sigma^{4/3} \frac{\beta x_\sigma^2}{1 + 6\beta x_\sigma \sinh^{-1} x_\sigma} d^3\mathbf{r} && \text{(A.3)} \\ &= E_X(2/3) - \sum_\sigma \int \rho_\sigma^{4/3} \beta x_\sigma^2 h(x_\sigma) d^3\mathbf{r} && \text{(A.4)} \end{aligned}$$

where

$$x_\sigma(\rho_\sigma, \nabla\rho_\sigma) = \frac{|\nabla\rho_\sigma|}{\rho_\sigma^{4/3}}$$

and $\beta = 0.0042$ a.u.

$$E_{B88} = \sum_\sigma \int \rho_\sigma^{4/3}\left\{-\frac{3}{2}\left(\frac{3}{4\pi}\right)^{1/3} - \beta x_\sigma^2 h(x_\sigma)\right\} d^3\mathbf{r} = \sum_\sigma \int \rho_\sigma^{4/3} g(x_\sigma) d^3\mathbf{r} \tag{A.5}$$

This form leads to the corresponding expression for the exchange potential

$$\begin{aligned} V_{B88} &= -\left(\frac{3}{\pi}\right)^{1/3} 2^{-2/3}\sum_\sigma \rho_\sigma^{1/3} \\ &\quad -\beta\sum_\sigma \rho_\sigma^{-4/3} h(x_\sigma)\left\{\frac{4}{3}x_\sigma^2\rho^{5/3} - \nabla^2\rho_\sigma\left[1 + h(x_\sigma)\left(1 - \frac{6\beta x_\sigma^2}{\sqrt{1+x_\sigma^2}}\right)\right]\right. \\ &\qquad +6\beta h(x_\sigma)\nabla\rho_\sigma\cdot\nabla x_\sigma\left[(1 + 2h(x_\sigma))\sinh^{-1} x_\sigma\right. \\ &\qquad \left.\left. + \frac{x_\sigma}{\sqrt{1+x_\sigma^2}}\left(\frac{1}{1+x_\sigma^2} + 2h(x_\sigma)\left(2 - \frac{6\beta x_\sigma^2}{\sqrt{1+x_\sigma^2}}\right)\right)\right]\right\} \end{aligned} \tag{A.6}$$

Appendix A.3. PW86 exchange potential

According to Perdew and Wang [**?**]

$$E_{PW86} = \frac{1}{2}\sum_{\sigma} E(2\rho_\sigma) \tag{A.7}$$

$$E(\rho) = A_x \int \rho^{4/3}(1 + as^2 + bs^4 + cs^6)^m d\mathbf{r}^3 = A_x \int \rho^{4/3} F(s)$$

where $A_x = -\frac{3}{4}(3/\pi)^{1/3}$, $F(s) = (1 + as + bs + cs)^m = F_0^m(s)$, $a = 1.296$, $b = 14$, $c = 0.2$, $m = 1/15$, $k_F = (3\pi^2\rho)^{1/3}$ and

$$s = \frac{|\nabla\rho|}{2k_F\rho} = \frac{|\nabla\rho|/\rho^{4/3}}{(24\pi^2)^{1/3}}$$

According to the user's manual of the MOLPRO program (http://wild.life.nctu.edu.tw/~jsyu/molpro2002.1/doc/manual/manual.html)

$$s = \frac{|\nabla\rho|/\rho^{4/3}}{(48\pi^2)^{1/3}}.$$

This discrepancy is due to the different definition of ρ: $\rho = 2\rho_\sigma$ and $\rho = \rho_\sigma$ in the two respective cases.

Eq. (**??**) leads to the following expresion for the potential

$$V_{PW86} = \frac{1}{2}\sum_{\sigma} V(2\rho_\sigma) \tag{A.8}$$

$$V(\rho) = A_x\rho^{1/3}\left\{\frac{4}{3}F - ts^{-1}\frac{dF}{ds} - \left(u - \frac{4}{3}s^3\right)\frac{d}{ds}\left(s^{-1}\frac{dF}{ds}\right)\right\}$$

where

$$t = (2k_F)^{-2}\rho^{-1}\nabla^2\rho$$

$$u = (2k_F)^{-3}\rho^{-2}\nabla\rho\cdot\nabla|\nabla\rho|$$

and

$$|\nabla\rho| = (\nabla\rho\cdot\nabla\rho)^{1/2}$$

$$\frac{dF}{ds} = m(1 + as^2 + bs^4 + cs^6)^{m-1}(2as + 4bs^3 + 6cs^5) = m{F_0}^{m-1}\frac{dF_0}{ds}$$

$$\frac{d}{ds}\left(s^{-1}\frac{dF}{ds}\right) = mF_0^{m-2}\left[(8bs + 24cs^3)F_0 + (m-1)s^{-1}\left(\frac{F_0}{ds}\right)^2\right]$$

Appendix A.4. PW91 exchange potential

According to Perdew [**?**] the exchange energy can be approximated by the following formula

$$E_{PW91} = \frac{1}{2}\sum_{\sigma} E(2\rho_\sigma) \tag{A.9}$$

$$E(\rho) = -\frac{3}{4}\left(\frac{3}{\pi}\right)^{1/3}\rho^{4/3}F(s)$$

$$F(s) = \frac{1 + a_1 s\sinh^{-1}(as) + (a_2 - a_3\exp(-a_4 s^2))\,s^2}{1 + a_1 s\sinh^{-1}(as) + b_1 s^4} \tag{A.10}$$

where $a_1 = 0.19645$, $a = 7.7956$, $a_2 = 0.2743$, $a_3 = 0.1508$, $a_4 = 100$, $b_1 = 0.004$ and

$$s = \frac{|\nabla\rho|/\rho^{4/3}}{(24\pi^2)^{1/3}}.$$

$\sinh^{-1}(x)$ can be calculated as $\log(x + \sqrt{1 + x^2})$.

Appendix A.5. LYP correlation potential

The correlation correction energy of an electron gas distribution characterized by ρ_α and ρ_β densities is calculated according to Eq. (22) of Lee, Yang and Parr [**?**], namely

$$\begin{aligned} E_{LYP} = -a\int \frac{\gamma}{1 + d\rho^{-1/3}}\{\rho + 2b\rho^{-5/3}[2^{2/3}C_F(\rho_\alpha^{8/3} + \rho_\beta^{8/3}) - \rho t_W \\ + \frac{1}{9}(\rho_\alpha t_W(\rho_\alpha) + \rho_\beta t_W(\rho_\beta)) \\ + \frac{1}{18}(\rho_\alpha\nabla^2\rho_\alpha + \rho_\beta\nabla^2\rho_\beta)]e^{-c\rho^{-1/3}}\} \end{aligned} \tag{A.11}$$

where $a = 0.04918$, $b = 0.132$, $c = 0.2533$, $d = 0.349$, $C_F = \frac{3}{10}(3\pi^2)^{2/3}$,

$$\gamma = 2\left[1 - \frac{\rho_\alpha^2 + \rho_\beta^2}{\rho^2}\right], \qquad \rho = \rho_\alpha + \rho_\beta$$

$$t_W(n) = \frac{1}{8}\left[\frac{|\nabla n|^2}{n} - \nabla^2 n\right], \qquad n = \rho, \rho_\alpha, \rho_\beta$$

$$\begin{aligned} V_{LYP} = -a(F_1'\rho + F_1) - abC_F\rho^{5/3}(G_1'\rho + \frac{8}{3}G_1) \\ -\frac{ab}{4}\left[G_1''\rho|\nabla\rho|^2 + G_1'(3|\nabla\rho|^2 + 2\rho\nabla^2\rho) + 4G_1\nabla^2\rho\right] \\ -\frac{ab}{72}\left[3G_1''\rho|\nabla\rho|^2 + G_1'(5|\nabla\rho|^2 + 6\rho\nabla^2\rho) + 4G_1\nabla^2\rho\right] \end{aligned} \tag{A.12}$$

where $G_1 = F_1\rho^{-5/3}e^{-c\rho^{-1/3}}$, $F_1^{-1} = 1 + d\rho^{-1/3}$ and $|\nabla^2\rho| = \nabla\rho \cdot \nabla\rho$.

The potential for a closed-shell case can be expressed via F_1 as

$$\begin{aligned} V_{LYP} = &-\frac{ad}{3}\rho^{-1/3}F_1^2 - aF_1 \\ &-abC_F F_1 g_0 \rho^{5/3}\left(g_2 + \frac{8}{3}\right) \\ &-\frac{19}{18}abF_1 g_0 \nabla^2\rho \\ &-\frac{ab}{72}F_1 g_0 g_2\left(42\nabla^2\rho + 59\rho^{-1}|\nabla\rho|^2\right) \\ &-\frac{7}{24}abF_1 g_0 \rho^{-1}|\nabla\rho|^2\left[g_2\left(\frac{d}{3}F_1\rho^{-1/3} + g_1 - 1\right) + \frac{1}{9}g_3\rho^{-1/3}\right] \end{aligned} \tag{A.13}$$

where

$$
\begin{aligned}
g_0(\rho) &= \rho^{-5/3} e^{-c\rho^{-1/3}} & \frac{dg_0}{d\rho} &= g_0 g_1 \rho^{-1} \\
g_1 &= -\frac{5}{3} + \frac{c}{3}\rho^{-1/3} & \frac{dg_1}{d\rho} &= -\frac{c}{9}\rho^{-4/3} \\
g_2(\rho) &= \frac{d}{3}F_1\rho^{-1/3} + g_1 & \frac{dg_2}{d\rho} &= \frac{1}{9}g_3\rho^{-4/3} \\
g_3(\rho) &= d^2F_1^2\rho^{-1/3} - dF_1 - c & \frac{dF_1}{d\rho} &= \frac{d}{3}F_1^2\rho^{-4/3} \\
G_1(\rho) &= F_1 g_0 & \frac{dG_1}{d\rho} &= F_1 g_0 g_2 \rho^{-1}
\end{aligned}
$$

Appendix A.6. VWN correlation potential

The VWN correlation functional [**?**] is defined as

$$E_{VWN} = \int \rho(r) q_{klmn}(x) dr \tag{A.14}$$

where $x = \left(\frac{3}{4\pi}\right)^{1/6} \rho(r)^{-1/6}$ and $q_{klmn}(x)$ is given by

$$
\begin{aligned}
q_{Apcd}(x) &= A\left\{\ln\frac{x^2}{X(x,c,d)} + \frac{2c}{Q(c,d)}\arctan\left(\frac{Q(c,d)}{2x+x}\right)\right. \\
&\quad \left. -\frac{cp}{X(p,c,d)}\left(\ln\frac{x-p}{X(x,c,d)} + 2\frac{c+2p}{Q(c,d)}\arctan\left(\frac{Q(c,d)}{2x+x}\right)\right)\right\} \\
Q(c,d) &= \sqrt{4d-c^2} \\
X(i,c,d) &= i^2 + ic + d
\end{aligned}
$$

This formuala is valid for a closed-shell system and the parameters k, l, m, n are equal 0.0310907, -0.10498, 3.72744 and 12.9352, respectively (cf. http://-wild.life.nctu.edu.tw/~jsyu/molpro2002.1/doc/manual/node184.html), and leads to the following expression for the correlation potential

$$V(r) = q_{klmn}(x) + \rho(r)\frac{dx}{d\rho}\frac{dq_{klmn}(x)}{dx} \tag{A.15}$$

where

$$\begin{aligned}
\frac{dx}{d\rho} &= -\frac{1}{8\pi}\left(\frac{4\pi}{3}\right)^{5/6}\rho^{-7/6} \\
\frac{dq_{Apcd}}{dx} &= A\left\{\frac{2}{x} - \frac{X'(x,c,d)}{X(x,c,d)} - \frac{4c}{Q(d,c)^2 + X'(x,c,d)^2}\right. \\
&\quad + \frac{4cp(c+2p)}{X(p,c,d)(Q(d,c)^2 + X'(x,c,d)^2)} \\
&\quad \left. - \frac{cp}{X(p,c,d)}\left(\frac{2}{x-p} - \frac{X'(x,c,d)}{X(x,c,d)}\right)\right\}
\end{aligned}$$

and $X'(x,c,d) = \partial X/\partial x = 2x + c$.

Appendix A.7. Differential operators in prolate spheroidal coordinates

When perfoming DFT calculations using generalized gradient approximation one needs to evaluate $\nabla^2 f$ and $\nabla f \nabla g$ in the (transformed) prolate spheroidal coordinates where $f(x,y,z)$ and $g(x,y,z)$ functions are densities (or functions thereof) and thus are symmetric (i.e. m_a in Eq. (**??**) is zero). In order to help the reader to follow, check or modify the code responsible for evaluation of various DFT potentials used in the x2dhf program several relevant formulae have been collected below. Employing the definitions of prolate spheroidal coordinates as defined by Eqs (**??**), (**??**) and (**??**) one can write

$$\frac{\partial f}{\partial x} = \frac{\partial \xi}{\partial x}\frac{\partial \mu}{\partial \xi}\frac{\partial f}{\partial \mu} + \frac{\partial \eta}{\partial x}\frac{\partial \nu}{\partial \eta}\frac{\partial f}{\partial \nu}$$

$$\frac{\partial f}{\partial y} = \frac{\partial \xi}{\partial y}\frac{\partial \mu}{\partial \xi}\frac{\partial f}{\partial \mu} + \frac{\partial \eta}{\partial y}\frac{\partial \nu}{\partial \eta}\frac{\partial f}{\partial \nu}$$

$$\frac{\partial f}{\partial z} = \frac{\partial \xi}{\partial z}\frac{\partial \mu}{\partial \xi}\frac{\partial f}{\partial \mu} + \frac{\partial \eta}{\partial z}\frac{\partial \nu}{\partial \eta}\frac{\partial f}{\partial \nu}$$

$$\frac{\partial \mu}{\partial x} = \frac{1}{\sqrt{\xi^2-1}}\frac{\partial \xi}{\partial x} \qquad \frac{\partial \mu}{\partial y} = \frac{1}{\sqrt{\xi^2-1}}\frac{\partial \xi}{\partial y} \qquad \frac{\partial \mu}{\partial z} = \frac{1}{\sqrt{\xi^2-1}}\frac{\partial \xi}{\partial z}$$

$$\frac{\partial \nu}{\partial x} = \frac{-1}{\sqrt{1-\eta^2}}\frac{\partial \eta}{\partial x} \qquad \frac{\partial \nu}{\partial y} = \frac{-1}{\sqrt{1-\eta^2}}\frac{\partial \eta}{\partial y} \qquad \frac{\partial \nu}{\partial z} = \frac{-1}{\sqrt{1-\eta^2}}\frac{\partial \eta}{\partial z}$$

$$\frac{\partial \xi}{\partial x} = \frac{4}{R^2(\xi^2-\eta^2)}\xi x \qquad \frac{\partial \xi}{\partial y} = \frac{4}{R^2(\xi^2-\eta^2)}\xi y \qquad \frac{\partial \xi}{\partial z} = \frac{4}{R^2(\xi^2-\eta^2)}(\xi z - \frac{1}{2}R\eta)$$

$$\frac{\partial \eta}{\partial x} = \frac{-4}{R^2(\xi^2-\eta^2)}\eta x \qquad \frac{\partial \eta}{\partial y} = \frac{-4}{R^2(\xi^2-\eta^2)}\eta y \qquad \frac{\partial \eta}{\partial z} = \frac{-4}{R^2(\xi^2-\eta^2)}(\eta z - \frac{1}{2}R\xi)$$

$$\begin{aligned}
\frac{\partial f}{\partial x} &= \frac{4}{R^2(\xi^2-\eta^2)}\left\{\frac{\xi x}{\sqrt{\xi^2-1}}\frac{\partial f}{\partial \mu} + \frac{\eta x}{\sqrt{1-\eta^2}}\frac{\partial f}{\partial \nu}\right\} \\
\frac{\partial f}{\partial y} &= \frac{4}{R^2(\xi^2-\eta^2)}\left\{\frac{\xi y}{\sqrt{\xi^2-1}}\frac{\partial f}{\partial \mu} + \frac{\eta y}{\sqrt{1-\eta^2}}\frac{\partial f}{\partial \nu}\right\} \\
\frac{\partial f}{\partial z} &= \frac{4}{R^2(\xi^2-\eta^2)}\left\{\frac{(\xi z - \frac{1}{2}R\eta)}{\sqrt{\xi^2-1}}\frac{\partial f}{\partial \mu} + \frac{(\eta z - \frac{1}{2}R\xi)}{\sqrt{1-\eta^2}}\frac{\partial f}{\partial \nu}\right\}
\end{aligned}$$

$$\begin{aligned}
\frac{\partial f}{\partial x}\frac{\partial g}{\partial x} &= \left[\frac{4}{R^2(\xi^2-\eta^2)}\right]^2\left\{\frac{\xi^2}{(\xi^2-1)}\frac{\partial f}{\partial \mu}\frac{\partial g}{\partial \mu} + \frac{\eta^2}{(1-\eta^2)}\frac{\partial f}{\partial \nu}\frac{\partial g}{\partial \nu}\right. \\
&\qquad \left. + \frac{\xi\eta}{\sqrt{\xi^2-1}\sqrt{1-\eta^2}}\left(\frac{\partial f}{\partial \mu}\frac{\partial g}{\partial \nu} + \frac{\partial f}{\partial \nu}\frac{\partial g}{\partial \mu}\right)\right\} x^2
\end{aligned}$$

$$\begin{aligned}
\frac{\partial f}{\partial y}\frac{\partial g}{\partial y} &= \left[\frac{4}{R^2(\xi^2-\eta^2)}\right]^2\left\{\frac{\xi^2}{(\xi^2-1)}\frac{\partial f}{\partial \mu}\frac{\partial g}{\partial \mu} + \frac{\eta^2}{(1-\eta^2)}\frac{\partial f}{\partial \nu}\frac{\partial g}{\partial \nu}\right. \\
&\qquad \left. + \frac{\xi\eta}{\sqrt{\xi^2-1}\sqrt{1-\eta^2}}\left(\frac{\partial f}{\partial \mu}\frac{\partial g}{\partial \nu} + \frac{\partial f}{\partial \nu}\frac{\partial g}{\partial \mu}\right)\right\} y^2
\end{aligned}$$

$$\begin{aligned}
\frac{\partial f}{\partial z}\frac{\partial g}{\partial z} &= \left[\frac{4}{R^2(\xi^2-\eta^2)}\right]^2\left\{\frac{(\xi z - \frac{R}{2}\eta)^2}{(\xi^2-1)}\frac{\partial f}{\partial \mu}\frac{\partial g}{\partial \mu} + \frac{(\eta z - \frac{R}{2}\xi)^2}{(1-\eta^2)}\frac{\partial f}{\partial \nu}\frac{\partial g}{\partial \nu}\right. \\
&\qquad \left. + \frac{(\xi z - \frac{R}{2}\eta)(\eta z - \frac{R}{2}\xi)}{\sqrt{\xi^2-1}\sqrt{1-\eta^2}}\left(\frac{\partial f}{\partial \mu}\frac{\partial g}{\partial \nu} + \frac{\partial f}{\partial \nu}\frac{\partial g}{\partial \mu}\right)\right\}
\end{aligned}$$

Since $x^2 + y^2 = \frac{R^2}{4}(\xi^2 - 1)(1 - \eta^2)$

$$
\begin{aligned}
\nabla f \nabla g &= \left[\frac{4}{R^2(\xi^2 - \eta^2)}\right]^2 \\
&\left\{\left(\frac{R^2}{4}\xi^2(1-\eta^2) + \frac{(\xi z - \frac{R}{2}\eta)^2}{(\xi^2-1)}\right)\frac{\partial f}{\partial \mu}\frac{\partial g}{\partial \mu} + \right. \\
&\left(\frac{R^2}{4}\eta^2(1-\xi^2) + \frac{(\eta z - \frac{R}{2}\xi)^2}{(1-\eta^2)}\right)\frac{\partial f}{\partial \nu}\frac{\partial g}{\partial \nu} + \\
&\left.\left(\frac{R^2}{4}\xi\eta\sqrt{\xi^2-1}\sqrt{1-\eta^2} + \frac{(\xi z - \frac{R}{2}\eta)(\eta z - \frac{R}{2}\xi)}{\sqrt{\xi^2-1}\sqrt{1-\eta^2}}\right)\left(\frac{\partial f}{\partial \mu}\frac{\partial g}{\partial \nu} + \frac{\partial f}{\partial \nu}\frac{\partial g}{\partial \mu}\right)\right\} \\
\nabla^2 f &= \frac{4}{R^2(\xi^2-\eta^2)}\left(\frac{\partial^2 f}{\partial \mu^2} + \frac{\xi}{\sqrt{\xi^2-1}}\frac{\partial f}{\partial \mu} + \frac{\partial^2 f}{\partial \nu^2} + \frac{\eta}{\sqrt{1-\eta^2}}\frac{\partial f}{\partial \nu}\right)
\end{aligned}
$$

Appendix A. Finite nucleus models

In contemporary investigations of nuclear structure in neutron scattering experiments two representations of the nuclear structure are most often used: a Fourier-Bessel expansion and a linear combination of (distributed) Gaussian functions, whose adjustable parameters are refined to allow for an accurate description of the nuclear charge distribution deduced from experimental studies [**?**]. It is, however, an established practice to use simpler empirical models in atomic and molecular electronic structure calculation, of which the uniform charge distribution, the Gaussian and Fermi models are encountered most often in electronic structure theory. A detailed discussion of different nuclear charge distribution models has been recently published by D. Andrae [**?**].

We assume that the nuclear charge distribution is spherically symmetrical and can be written in the form

$$V(r) = -\frac{Z(r)}{r}, \quad r > 0$$

The x2dhf program implements two simple parametric nuclear models: the Gaussian nuclear model and the Fermi nuclear model.

Appendix A.1. Gaussian nuclear model

The Gaussian nuclear charge distribution has the form

$$\rho(r) = Z\left(\frac{\lambda}{\pi}\right)^{\frac{3}{2}} \exp\left(-\lambda r^2\right)$$

where the exponent of the normalized Gaussian-type function representing the nuclear distribution is determined by the root-mean-square radius of the nuclear charge distribution via the relation $\lambda = 3/2\left\langle r^2\right\rangle$. A statistical model gives the following value for the root-mean-square radius (in fm)

$$\left\langle r^2\right\rangle^{1/2} = 0.836A^{1/3} + 0.570, \qquad A > 6 \tag{A.1}$$

where A is the atomic mass of a nucleus. Therefore, when the distance is expressed in atomic units we have

$$\lambda = \frac{3}{2}10^{10}\left(\frac{0.529177249}{0.836A^{\frac{1}{3}} + 0.570}\right)^2$$

For any spherically symmetric charge distribution $\rho(r)$ the potential energy is

$$-rV(r) = 4\pi\left(\int_0^r s^2\rho(s)ds + r\int_r^\infty s\rho(s)ds\right)$$

If $\rho(r) = \rho_0\exp(-\lambda r^2)$ then the first integral is equal to

$$\rho_0\left(\frac{-r\exp(-\lambda r^2)}{2\lambda} + \frac{\sqrt{\pi}\mathrm{erf}(\sqrt{\lambda}r)}{4\lambda^{3/2}}\right)$$

and the second to $\rho_0 r\exp(-\lambda r^2)/2\lambda$. Thus

$$\begin{aligned} -rV(r) &= \rho_0\left(\frac{\pi}{\lambda}\right)^{3/2}\mathrm{erf}\left(\sqrt{\lambda}r\right) = Z\mathrm{erf}\left(\sqrt{\lambda}r\right) \\ &= \frac{2Z}{\sqrt{\pi}}\left(\gamma\left(\frac{3}{2},\eta r^2\right) + \sqrt{\eta}re^{-\eta r^2}\right) \\ &= \frac{2Z}{\sqrt{\pi}}\left(\gamma\left(\frac{3}{2},\eta r^2\right) + \sqrt{\eta}r\left(1-\gamma(1,\eta r^2)\right)\right) \end{aligned}$$

since $\rho_0 = Z(\lambda/\pi)^{3/2}$ (the last form of the potential can be found in Parpia's paper [**?**]). This potential reduces to the Coulomb potential if $r \gg \sqrt{\lambda}$. In

case a very tight diatomic system with finite nuclei is considered the $Z_1 Z_2/r$ contribution to the total energy must be replaced by

$$\frac{Z_1 Z_2}{r} \frac{1}{\sqrt{\pi}} \gamma \left(\frac{1}{2}, \lambda_{12} r^2 \right)$$

where $\gamma(a, x)$ is the lower incomplete gamma function

$$\gamma(a, x) = \int_0^x t^{a-1} e^{-t} dt \tag{A.2}$$

and $1/\lambda_{12} = 1/\lambda_1 + 1/\lambda_2$ [**?**].

Appendix A.2. Fermi nuclear model

The Fermi nuclear model contains more detail concerning the charge distribution than the Gaussian model and has traditionally been employed in fitting nuclear scattering data. The *Fermi nucleus* has the form of a Fermi distribution

$$\rho(r) = \frac{\rho_0}{1 + e^{(r-c)/a}}$$

where c is the *half-density radius* since $\rho(c) = \rho_0/2$. The parameter a is related to the nuclear *skin thickness* t through $t/a = 4 \ln 3$. It may be verified that $\rho(c - t/2) = 0.9\rho_0$ and that $\rho(c + t/2) = 0.1\rho_0$. The skin thickness is thus the interval across which the nuclear charge density drops from $0.9\rho_0$ to $0.1\rho_0$. It is a standard practice to take $t = 2.30$ fm independent of the atomic mass. The parameter c depends on the atomic mass through Eq. (**??**) and the following relation

$$\left\langle r^2 \right\rangle \approx \frac{3}{5} c^2 + \frac{7}{5} \pi^2 a^2$$

The Fermi nuclear potential reads

$$\begin{aligned} -rV(r) &= \frac{Z}{N} \left\{ 6 \left(\frac{a}{c} \right)^3 \left[-S_3 \left(-\frac{c}{a} \right) + S_3 \left(\frac{r-c}{a} \right) \right] \right. \\ &\left. + \frac{r}{c} \left[\frac{3}{2} + \frac{1}{2} \pi^2 \left(\frac{a}{c} \right)^2 - 3 \left(\frac{a}{c} \right)^2 S_2 \left(\frac{r-c}{a} \right) - \frac{1}{2} \left(\frac{r}{c} \right)^2 \right] \right\} \end{aligned}$$

for $r/c < 1$ and

$$-rV(r) = \frac{Z}{N} \left\{ N + 3 \left(\frac{a}{c} \right)^2 \left[\frac{r}{c} S_2 \left(\frac{r-c}{a} \right) + 2 \left(\frac{a}{c} \right) S_3 \left(\frac{r-c}{a} \right) \right] \right\}$$

otherwise; $N = 1 + \pi^2(a/c)^2 - 6(a/c)^3 S_3(-c/a)$ and S_k is an infinite series defined as

$$S_k(r) = \sum_{n=1}^{\infty} (-1)^n \frac{e^{nr}}{n^k}$$

This is the potential for the Fermi charge distribution used in GRASP2 package [**?**] and the x2dhf program follows suit.

Appendix A. Miscelenous formulae

Recursive formula for the Legendre polynomials

$$P_{n+1}(z) = \frac{1}{n+1} \left[(2n+1) z P_n(z) - n P_{n-1}(z) \right]$$

Recursive formulae for the associate Legendre polynomials

$$\begin{aligned} P^q_{k+1} &= \frac{1}{k-q+1} \left[(2k+1) z P^q_k(z) - (k+q) P^q_{k-1}(z) \right] \\ P^q_k &= \frac{(-1)^q \Gamma(k+q+1)(1-z^2)^{q/2}}{2^q \Gamma(k-q+1) q!} F\left(q-k, q_k+1; q+1; \frac{1-z}{2} \right) \end{aligned}$$

The program uses the following associate Legrendre polynomials to calculate boundary values from the multipole expansion:

$$
\begin{aligned}
P_1^1(z) &= -\frac{1}{\sqrt{2}}\sqrt{1-z^2} \\
P_2^1(z) &= -\frac{3}{\sqrt{6}}z\sqrt{1-z^2} \\
P_3^1(z) &= \frac{3}{2\sqrt{12}}(1-5z^2)\sqrt{1-z^2} \\
P_4^1(z) &= \frac{5}{2\sqrt{20}}(3z-7z^3)\sqrt{1-z^2} \\
P_5^1(z) &= \frac{15}{8\sqrt{30}}(-1+14z^2-21z^4)\sqrt{1-z^2} \\
P_6^1(z) &= \frac{21}{8\sqrt{42}}(-5z+30z^3-33z^5)\sqrt{1-z^2} \\
P_7^1(z) &= \frac{7}{16\sqrt{56}}(5-135z^2+495z^4-429z^6)\sqrt{1-z^2} \\
P_8^1(z) &= \frac{9}{16\sqrt{72}}(35z-385z^3+1001z^5-715z^7)\sqrt{1-z^2}
\end{aligned}
$$

$$
\begin{aligned}
P_2^2(z) &= \frac{3}{\sqrt{24}}(1-z^2) \\
P_3^2(z) &= \frac{15}{\sqrt{120}}(z-z^3) \\
P_4^2(z) &= \frac{15}{2\sqrt{360}}(-1+8z^2-7z^4) \\
P_5^2(z) &= \frac{105}{2\sqrt{840}}(-z+4z^3-3z^5) \\
P_6^2(z) &= \frac{108}{2\sqrt{1680}}(1-19z^2+51z^4-33z^6) \\
P_7^2(z) &= \frac{63}{8\sqrt{3024}}(15z-125z^3+253z^5-143z^7) \\
P_8^2(z) &= \frac{315}{8\sqrt{5040}}(-1+34z^2-176z^4+286z^6-143z^8)
\end{aligned}
$$

$$
\begin{aligned}
P_3^3(z) &= \frac{15}{\sqrt{720}}(-1+z^2)\sqrt{1-z^2} \\
P_4^3(z) &= \frac{105}{\sqrt{5040}}z(-1+z^2)\sqrt{1-z^2} \\
P_5^3(z) &= \frac{105}{2\sqrt{20160}}(-1+9z^2)(-1+z^2)\sqrt{1-z^2} \\
P_6^3(z) &= \frac{315}{2\sqrt{60480}}(-3z+11z^3)(-1+z^2)\sqrt{1-z^2} \\
P_7^3(z) &= \frac{315}{8\sqrt{151200}}(3-66z^2+143z^4)(-1+z^2)\sqrt{1-z^2} \\
P_8^3(z) &= \frac{3465}{8\sqrt{332640}}(3z-26z^3+39z^5)(-1+z^2)\sqrt{1-z^2}
\end{aligned}
$$

$$
\begin{aligned}
P_4^4(z) &= \frac{105}{\sqrt{40320}}(1-2z^2+z^4) \\
P_5^4(z) &= \frac{945}{\sqrt{362880}}(z-2z^3+z^5) \\
P_6^4(z) &= \frac{945}{2\sqrt{1814400}}(-1+13z^2-23z^4+11z^6) \\
P_7^4(z) &= \frac{3465}{2\sqrt{6652800}}(-3z+19z^3-29z^5+13z^7) \\
P_8^4(z) &= \frac{10395}{8\sqrt{19958400}}(1-28z^2+118z^4-156z^6+65z^8)
\end{aligned}
$$

The first and second derivatives are approximated by 9-point finite difference formulae derived from the following Stirling central difference formula

$$
\begin{aligned}
f(x) = f(x_0+uh) &= f(x_0) + uN_1f(x_0) + \frac{u^2}{2!}\delta^2 f(x_0) + \frac{u(u^2-1)}{3!}N_3 f(x_0) + \ldots \\
&\quad + \frac{u(u^2-1)(u^2-2^2)\ldots(u^2-(p-1)^2)}{(2p-1)!}N_{2p-1}f(x_0) \\
&\quad + \frac{u^2(u^2-1)(u^2-2^2)\ldots(u^2-(p-1)^2)}{(2p)!}\delta^{2p}f(x_0)
\end{aligned}
$$

where

$$\begin{aligned} \delta f(x_0) &= f(x_0 + h/2) - f(x_0 - h/2) \\ \delta^k f(x_0) &= \delta\left(\delta^{k-1} f(x_0)\right) \\ N_k f(x_0) &= \frac{1}{2}\left(\delta^k f(x_0 + h/2) + \delta^k f(x_0 - h/2)\right) \end{aligned}$$

References

[] F. Jensen, Introduction to computational chemistry, Wiley, New York, 1999.

[] E. L. Albasiny, J. R. A. Cooper, Mol. Phys. 4 (1961) 353–358.

[] E. L. Albasiny, J. R. A. Cooper, Proc. Phys. Soc. 82 (1963) 289–303.

[] E. L. Albasiny, J. R. A. Cooper, Proc. Phys. Soc. 85 (1965) 1133–1142.

[] E. L. Albasiny, J. R. A. Cooper, Proc. Phys. Soc. 88 (1966) 315–323.

[] J. A. Keefer, J. K. Su Fu, R. L. Belford, J. Chem. Phys. 50 (1969) 160–173.

[] A. D. Becke, R. M. Dickson, J. Chem. Phys. 89 (1988) 2993–2997.

[] A. D. Becke, R. M. Dickson, J. Chem. Phys. 92 (1990) 3610–3612.

[] R. M. Dickson, A. D. Becke, J. Chem. Phys. 99 (1993) 3898–3905.

[] T. Shiozaki, S. Hirata, Phys. Rev. A 76 (2007) 040503.

[] E. A. McCullough Jr., Chem. Phys. Lett. 24 (1974) 55–58.

[] E. A. McCullough Jr., Comput. Phys. Rep. 4 (1986) 265–312.

[] A. D. Becke, J. Chem. Phys. 76 (1982) 6037–6045.

[] A. D. Becke, J. Chem. Phys. 78 (1983) 4787–4788.

[] A. D. Becke, Int. J. Quantum Chem. 27 (1985) 585.

[] A. D. Becke, Phys. Rev. A 33 (1986) 2786.

[] A. N. Artemyev, E. V. Ludeña, V. Karasiev, A. J. Hernandez, J. Comput. Chem. 25 (2003) 368–374.

[] D. Heinemann, D. Kolb, B. Fricke, Chem. Phys. Lett. 137 (1987) 180–182.

[] D. Heinemann, B. Fricke, D. Kolb, Phys. Rev. A 38 (1988) 4994–5001.

[] D. Heinemann, A. Rosén, B. Fricke, Physica Scripta 42 (1990) 692–696.

[] O. Beck, D. Heinemann, D. Kolb, Fast and accurate molecular Hartree-Fock with a finite-element multigrid method, 2003.

[] S. Hackel, D. Heinemann, D. Kolb, B. Fricke, Chem. Phys. Lett. 206 (1993) 91–95.

[] L. Yang, D. Heinemann, D. Kolb, Chem. Phys. Lett. 178 (1991) 213.

[] L. Yang, D. Heinemann, D. Kolb, Chem. Phys. Lett. 192 (1992) 499.

[] C. Düsterhöft, L. Yang, D. Heinemann, D. Kolb, Chem. Phys. Lett. 229 (1994) 667–670.

[] D. Sundholm, Comput. Phys. Commun. 49 (1988) 409.

[] D. Sundholm, J. Olsen, P. Malmqvist, B. O. Roos, in: M. Defranceschi, J. Delhalle (Eds.), Numerical determination of the electronic structure of atoms diatomic and polyatomic molecules, volume 271 of *NATO ASI Series, Series C: Mathematical and Physical Sciences*, Kluwer Academic Publishers, Dordrecht, 1989, pp. 329–334.

[] D. Sundholm, J. Olsen, Proc. 13th. IMACS World Congress on Computation and Applied Mathematics, Criterion, Dublin, 1991, p. 861.

[] J. C. Morrison, T. Wolf, B. Bialecki, G. F. Weather, L. Larson, Mol. Phys. 98 (2000) 1175–1184.

[] J. C. Morrison, S. Boyd, L. Marsano, B. Bialecki, T. Ericsson, J. P. Santos, Commun. Comput. Phys. 5 (2009) 959–985.

[] L. Laaksonen, P. Pyykkö, D. Sundholm, Comput. Phys. Rep. 4 (1986) 313–344.

[] K. Davstad, J. Chem. Phys. 99 (1992) 33–38.

[] T. Beck, Rev. Mod. Phys. 72 (2000) 1041–1080.

[] T. A. Arias, Rev. Mod. Phys. 71 (1999) 267.

[] J. Kobus, Chem. Phys. Lett. 202 (1993) 7–12.

[] J. Kobus, Comput. Phys. Commun. 78 (1994) 247–255.

[] J. Kobus, Adv. Quantum Chem. 28 (1997) 1–14.

[] J. Kobus, L. Laaksonen, D. Sundholm, Comput. Phys. Commun. 98 (1996) 346–358.

[] J. Kobus, in: S. Wilson, P. F. Bernath, R. McWeeny (Eds.), Handbook of Molecular Physics and Quantum Chemistry, volume 2, chap. 9, Wiley, Chichester, 2003.

[] D. Moncrieff, S. Wilson, Chem. Phys. Lett. 209 (1993) 423–426.

[] D. Moncrieff, S. Wilson, J. Phys. B: At. Mol. Opt. Phys. 26 (1993) 1605–1616.

[] J. Kobus, D. Moncrieff, S. Wilson, J. Phys. B: At. Mol. Opt. Phys. 27 (1994) 2867–2875.

[] J. Kobus, D. Moncrieff, S. Wilson, J. Phys. B: At. Mol. Opt. Phys. 27 (1994) 5139–5147.

[] J. Kobus, D. Moncrieff, S. Wilson, Mol. Phys. 86 (1995) 1315–1330.

[] D. Moncrieff, J. Kobus, S. Wilson, J. Phys. B: At. Mol. Opt. Phys. 28 (1995) 4555–4557.

[] D. Moncrieff, S. Wilson, J. Phys. B: At. Mol. Opt. Phys. 29 (1996) 2425–2451.

[] D. Moncrieff, J. Kobus, S. Wilson, Mol. Phys. 93 (1998) 713–725.

[] J. Kobus, D. Moncrieff, S. Wilson, Mol. Phys. 96 (1999) 1559–1567.

[] J. Kobus, D. Moncrieff, S. Wilson, Phys. Rev. A 62 (2000) 062503/1–9.

[] J. Kobus, D. Moncrieff, S. Wilson, Mol. Phys. 98 (2000) 401–408.

[] J. Kobus, D. Moncrieff, S. Wilson, Mol. Phys. 100 (2002) 499–508.

[] J. Kobus, D. Moncrieff, S. Wilson, J. Phys. B: At. Mol. Opt. Phys. 34 (2001) 5127–5143.

[] J. Kobus, D. Moncrieff, S. Wilson, J. Phys. B: At. Mol. Opt. Phys. 37 (2004) 571–585.

[] J. Kobus, D. Moncrieff, S. Wilson, J. Phys. B: At. Mol. Opt. Phys. 40 (2007) 877–896.

[] J. Kobus, Comp. Lett. 3 (2007) 71–113.

[] J. Kobus, Special Volume of the American Institute of Physics Conference Proceedings.

[] A. Halkier, W. Klopper, T. Halgaker, P. Jørgensen, J. Chem. Phys. 111 (1999) 4424–4430.

[] A. Halkier, T. Helgaker, P. Jørgensen, W. Klopper, J. Olsen, Chem. Phys. Lett. 302 (1999) 437–446.

[] K. Aa. Christensen, F. Jensen, Chem. Phys. Lett. 317 (2000) 400–403.

[] F. Jensen, J. Chem. Phys. 110 (1999) 6601–6605.

[] F. Jensen, Theor. Chem. Acc. 104 (2000) 484–490.

[] F. Jensen, J. Chem. Phys. 115 (2001) 9113.

[] F. Jensen, J. Chem. Phys. 116 (2002) 7372–7379.

[] F. Jensen, J. Chem. Phys. 117 (2002) 9234–9240.

[] S. Shahbazian, M. Zahedi, Theor. Chem. Acc. 113 (2005) 152–160.

[] T. G. Williams, N. J. DeYonker, A. K. Wilson, The Journal of Chemical Physics 128 (2008) 044101.

[] N. B. Balabanov, K. A. Peterson, J. Chem. Phys. 123 (2005) 064107.

[] A. Helgakier, W. Klopper, H. Koch, J. Noga, J. Chem. Phys. 106 (1997) 9639.

[] S. Zhong, E. C. Barnes, G. A. Petersson, The Journal of Chemical Physics 129 (2008) 184116.

[] F. Jensen, Theor. Chem. Acc. 113 (2005) 187–190.

[] S. C. A. Halkier, Chem. Phys. Lett. 346 (2001) 329–333.

[] F. Pawłowski, P. Jørgensen, C. Hättig, Chem. Phys. Lett. 391 (2004) 27–32.

[] J. Styszyński, Chem. Phys. Lett. 317 (2000) 351–359.

[] J. Styszyński, J. Kobus, Chem. Phys. Lett. 369 (2003) 441–448.

[] E. Matito, J. Kobus, , J. Styszyski, Chem. Phys. 321 (2005) 277–284.

[] A. K. Roy, A. J. Thakkar, Chem. Phys. Lett. 362 (2002) 428–434.

[] J. F. Ziegler, J. P. Biersack, U. Littmark, The Stopping and Range of Ions in Solids, Pergamon, New York, 1985.

[] K. Nordlund, N. Runeberg, D. Sundholm, Nucl. Instrum. Meth. B 132 (1997) 45–54.

[] J. Pruneda, E. Artacho, PHYSICAL REVIEW B 70 (2004).

[] V. Kuzmin, Nuclear Instruments and Methods in Physics Research Section B: Beam Interactions with Materials and Atoms 249 (2006) 113–17.

[] V. Kuzmin, Surface and Coatings Technology 201 (2007) 8388–8392.

[] C. B. Madsen, L. B. Madsen, Phys. Rev. A 74 (2006) 023403.

[] S. Liu, V. K. R. López-Boada, F. De Proft, Int. J. Quantum Chem. 69 (1998) 513–522.

[] E. V. Ludeña, V. V. K. R. López-Boada, E. Valderrama, J. Maldonado, J. Comp. Chem. 20 (1999) 155–183.

[] V. V. Karasiev, J. Mol. Struct. (THEOCHEM) 493 (1999) 21–28.

[] V. V. Karasiev, E. V. Ludeña, A. N. Artemyev, Phys. Rev. A 62 (2000) 062510.

[] V. V. Karasiev, E. V. Ludeña, Phys. Rev. A 65 (2002) 062510.

[] V. V. Karasiev, E. V. Ludeña, Phys. Rev. A 65 (2002) 032515.

[] V. V. Karasiev, The Journal of Chemical Physics 118 (2003) 8576–8583.

[] V. V. Karasiev, S. B. Trickey, F. E. Harris, Chem. Phys. 330 (2006) 216–223.

[] J. Kobus, H. Quiney, S. Wilson, J. Phys. B: At. Mol. Opt. Phys. 34 (2001) 2045–2056.

[] T. Dziubak, J. Matulewski, pra 79 (2009) 043404.

[] C. F. Fischer, The Hartree-Fock method for atoms. A numerical approach, Wiley, New York, 1977.

[] J. Stoer, R. Bulirsch, Introduction to numerical analysis, Springer-Verlag, New York, 1980.

[] W. G. Bickley, Math. Gazzette 25 (1941) 19.

[] M. Abramowitz, L. A. S. Stegun, Handbook of Mathematical Functions, Wiley, New York, 1977.

[] L. A. Hageman, D. M. Young, Applied iterative methods, Academic Press, New York, 1981.

[] B. Sobczak, Analysis of SOR convergence rate, M.Sc. Thesis, Toruń, 2002.

[] J. D. Power, Philos. Trans. R. Soc. London Ser. A 274 (1973) 663.

[] C. F. Fischer, Comput. Phys. Commun. 64 (1996) 431–454.

[] L. S. Blackford, J. Demmel, J. Dongarra, I. Duff, S. Hammarling, G. Henry, M. Heroux, L. Kaufman, A. Lumsdaine, A. Petitet, R. Pozo, K. Remington, R. C. Whaley, ACM Trans. Math. Soft. 28-2 (2002) 135–151.

[] A. D. Becke, Phys. Rev. A 88 (1988) 3098–3100.

[] C. Lee, W. Yang, R. Parr, Phys. Rev. B 37 (1988) 785–789.

[] S. H. Vosko, L. Wilk, M. Nusair, Can. J. Phys. 58 (1980) 1200.

[] K. Schwarz, Phys. Rev. B 5 (1972) 2466–2468.

[] A. E. S. Green, D. L. Sellin, A. S. Zachor, Phys. Rev. 184 (1969) 1–9.

[] A. D. Buckingham, Adv. Chem. Phys. 12 (1967) 107.

[] A. D. McLean, M. Yoshimine, J. Chem. Phys. 47 (1967) 1927.

[] G. Maroulis, J. Chem. Phys. 118 (2003) 2673–2687.

[] A. H. WAPSTRA, G. AUDI, Nucl. Phys. A 432 (1983) 1–54.

[] G. AUDI, A. H. WAPSTRA, Nucl. Phys. A 565 (1993) 1–65.

[] J. P. Perdew, W. Yue, Phys. Rev. B 33 (1986) 8800–8802.

[] J. P. Perdew, J. A. Chevary, S. H. Vosko, K. A. Jackson, M. R. Pederson, C. Fiolhais, Phys. Rev. B 46 (1992) 6671.

[] H. de Vries, C. W. de Jager, C. de Vries, At. Data Nucl. Data Tables 36 (1987) 495.

[] D. Andrae, Phys. Rep. 336 (2000) 414–525.

[] F. A. Parpia, J. Phys. B: At. Mol. Opt. Phys. 30 (1997) 3983–4001.

[] F. A. Parpia, C. Froese Fischer, I. P. Grant, Comput. Phys. Commun. 94 (1996) 249–271.

[] B. G. Johnson, P. M. W. Gill, J. A. Pople, J. Chem. Phys. 98 (1993) 5612–5626.

Table A.1:
Dependence of the number of SCF iterations (M) required to solve the FD HF equations for the hydrogen fluoride molecule on overrelaxation parameters for orbitals (ω_{orb}) and potentials (ω_{pot}) [**?**]. The calculations were carried out using the grid a [451×877/200] grid and the orbital energy threshold was set to 10^{-8} with the initial orbitals and potentials converged to 10^{-2}. Next to optimal values of overrelaxation parameters are 1.947 and 1.994, respectively.

ω_{orb}	ω_{pot}	M
1.650	1.700	23059
1.850	1.880	9212
1.940	1.890	8411
1.947	1.980	1696
1.927	1.987	1519
1.947	1.987	1217
1.950	1.989	1111
1.967	1.987	1095
1.947	1.994	1065

Table A.2: Dependence of the number of SOR iterations (total SOR) and the time (in seconds) required to solve the FD HF equations on the number of SOR iterations used to relax the orbitals and potentials in a single SCF iteration (SOR/SCF). The calculations were started using as initial estimates the orbitals and potentials converged to within 10^{-4} (in orbital energy) and were stopped when the largest differences in orbital energies between two successive SCF iteration were less than 10^{-10}.

SOR/SCF	5	10	15	20	30	40	50
Be [169 × 217/35]							
total SOR	1520	1670	1785	1840	1860	1960	2000
time	29.5	27.6	26.1	25.2	25.2	**21.5**	24.1
BO [169 × 223/40]							
total SOR	2730	2990	3285	3700	4260	4600	19450
time	310.1	**269.4**	276.2	295.9	312.6	344.1	1468.2
BO [265 × 361/40]							
total SOR	4555	4870	4935	4780	5160	6120	6750
time	1269.9	1080.5	1009.6	**922.7**	938.3	1073.9	1257.0

Table A.3: Dependence of the hydrogen ground state kinetic, nuclear and total energy on discretization errors ($r_\infty = 25$ bohr) when the exact 1 σ function is used. Discretization errors due to the kinetic energy operator are proportional to h^8, where h is equal to the step size in ν/μ variables ($h_\nu \approx h_\mu$). Integration errors are of the same order of magnitude. $|1 - \langle I \rangle|$ denotes the error of the 1σ normalization constant and $\frac{1}{2} - \langle T \rangle$, $-1 - \langle V_n \rangle$ and $-\frac{1}{2} - \langle T + V_n \rangle$ denote the absolute errors of the kinetic, nuclear and total energy, respectively.

$N_\nu \times N_\mu$	h^8	$\lvert 1 - \langle I \rangle \rvert$	$\frac{1}{2} - \langle T \rangle$	$-1 - \langle V_n \rangle$	$-\frac{1}{2} - \langle T + V_n \rangle$
7×7	6.4×10^{-2}	1.1×10^{-1}	-2.8×10^{-2}	2.1×10^{-2}	-7.0×10^{-3}
13×19	2.1×10^{-5}	1.9×10^{-5}	1.7×10^{-4}	-1.7×10^{-4}	1.7×10^{-6}
25×31	1.5×10^{-7}	3.6×10^{-6}	-2.6×10^{-6}	2.7×10^{-6}	1.1×10^{-9}
37×49	3.9×10^{-9}	2.3×10^{-8}	-3.3×10^{-8}	3.3×10^{-8}	4.0×10^{-11}
55×73	1.5×10^{-10}	1.4×10^{-10}	-4.8×10^{-10}	5.0×10^{-10}	1.6×10^{-12}
103×139	8.5×10^{-13}	7.4×10^{-13}	-2.7×10^{-12}	2.8×10^{-12}	5.1×10^{-14}

Table A.4: Dependence of the helium ground state energy and its virial ratio on the grid used by the FD HF method ($r_\infty = 25$ bohr). The accuracy of the 1 σ orbital is monitored by calculating the deviation of the total electronic dipole moment of the atom, μ_z, from its exact value. $\Delta\langle T + V_n\rangle$, $\Delta\langle V_C\rangle$ and $\Delta\langle T + V_n + V_C\rangle$ denote the errors of one- and two-electron contributions and their sum on a given grid as measured with respect to the values obtained on the largest of the grids, namely $-3.887\,448\,865\,512\,68$, $1.025\,768\,869\,897\,97$ and $-2.861\,679\,995\,614\,71$.

$N_\nu \times N_\mu$	$\lvert\mu_z - 2\rvert$	$\Delta\langle T + V_n\rangle$	$\Delta\langle V_C\rangle$	$\lvert\Delta\langle T + V_n + V_C\rangle\rvert$	$\lvert\langle V_n + V_C\rangle / \langle T\rangle - 2\rvert$
7×7	1.7×10^{-1}	1.9×10^{-1}	2.2×10^{-1}	3.2×10^{-2}	2.9×10^{-1}
13×13	4.9×10^{-3}	-4.0×10^{-3}	5.2×10^{-3}	1.2×10^{-3}	2.0×10^{-2}
25×25	3.4×10^{-5}	2.1×10^{-5}	-2.9×10^{-5}	8.2×10^{-6}	8.9×10^{-5}
31×37	9.5×10^{-7}	-5.7×10^{-6}	1.2×10^{-6}	4.4×10^{-6}	1.3×10^{-5}
43×49	2.7×10^{-8}	-5.6×10^{-9}	-7.0×10^{-8}	7.5×10^{-8}	4.7×10^{-7}
55×67	1.4×10^{-9}	-4.1×10^{-9}	-3.4×10^{-9}	7.5×10^{-9}	4.6×10^{-8}
67×79	1.6×10^{-10}	-1.1×10^{-9}	-4.3×10^{-10}	1.6×10^{-9}	9.0×10^{-9}
79×97	1.6×10^{-11}	-2.8×10^{-10}	-7.6×10^{-11}	3.6×10^{-10}	2.1×10^{-9}
91×109	1.8×10^{-11}	-9.5×10^{-11}	-2.4×10^{-11}	1.2×10^{-10}	6.9×10^{-10}
103×127	4.1×10^{-12}	-3.2×10^{-11}	-8.0×10^{-12}	4.0×10^{-11}	2.4×10^{-11}
121×145	2.2×10^{-12}	-9.7×10^{-12}	-3.0×10^{-12}	1.2×10^{-11}	6.6×10^{-11}
151×193	6.4×10^{-14}	-1.7×10^{-12}	-2.0×10^{-12}	3.3×10^{-12}	9.9×10^{-12}
217×265	1.2×10^{-13}	-1.3×10^{-13}	-1.8×10^{-13}	3.0×10^{-13}	4.2×10^{-13}
317×391	3.7×10^{-14}	0.0	0.0	0.0	8.8×10^{-13}

Table A.5: Comparison of FD energies (in au) for the GaF^{+39} one-electron system (R=3.353 bohr, [649×1129/200]) with the exact values from Power's program (OEDM) [**?**]. Orbitals are labeled with nlm triplet where n, l and m are the principal, orbital and magnetic quantum numbers, respectively.

nlm	OEDM	FD
100	−483.184 164 997 5	−483.184 164 997 9
210	−122.888 205 876 7	−122.888 205 876 8
200	−122.733 220 197 1	−122.733 220 197 1
320	−56.325 432 982 08	−56.325 432 982 09
310	−56.064 747 360 03	−56.064 747 360 04
300	−55.857 809 071 15	−55.857 809 071 16
430	−49.748 077 736 59	−49.748 077 736 62
540	−33.278 686 476 70	−33.278 686 476 95
420	−32.852 093 071 00	−32.852 093 071 00
211	−122.807 726 783 2	−122.807 726 783 2
321	−56.186 870 411 89	−56.186 870 411 65
311	−55.955 787 708 24	−55.955 787 708 00
431	−33.044 405 068 15	−33.044 405 068 14
322	−56.064 605 666 57	−56.064 605 666 58
432	−32.851 020 550 42	−32.851 020 550 43
422	−32.549 061 245 47	−32.549 061 245 47
433	−32.688 193 618 11	−32.688 193 618 11
543	−22.037 772 085 85	−22.037 772 085 85
533	−21.676 770 733 19	−21.676 770 733 15

Table A.6: Comparison of orbital (E_{orb}) and total (E_{tot}) energies of the Ca atom (in au) obtained by the one-dimensional (1D) and two-dimensional (2D) FD HF method (corresponding orbital labels are given in parentheses) [**?**]. Calculations were performed using the one- and two-dimensional grids defined as ρ_0=-18, h=0.0156, N=2500 and [451×859/200], respectively.

1D E_{orb}/E_{tot}		2D E_{orb}/E_{tot}	
−0.195 529 692 462	(4s)	−0.195 529 692 550	(6σ)
−1.340 706 956 90	(3p)	−1.340 706 956 98	($5\sigma/2\pi$)
−2.245 376 006 03	(3s)	−2.245 376 006 11	(4σ)
−13.629 269 206 5	(2p)	−13.629 269 206 6	($3\sigma/1\pi$)
−16.822 744 273 6	(2s)	−16.822 744 273 7	(2σ)
−149.363 725 893	(1s)	−149.363 725 893	(1σ)
−676.758 185 924		−676.758 185 926	

Table A.7: Comparison of total HF energies calculated by the finite difference (E_{FD}) method and the multigrid finite element (E_{FE}) method [**?**]. The FE results correspond to extrapolated values from a series of calculations performed on grids of increasing density [**?**]. [$N_\nu \times N_\mu / r_\infty$] denotes the FD grid. The FD results for the Be and LiH systems were taken from [**?**].

System	[$N_\nu \times N_\mu / r_\infty$]	E_{FD}	E_{FE}
LiH (R=3.015 au)	[259×433/150]	−7.987 352 237 23	−7.987 352 237 228
Be (R=2.386 au)	[349×643/200]	−14.573 023 168 3	−14.573 023 168 305
BH (R=2.336 au)	[349×643/200]	−25.131 598 702 3	−25.131 598 702 31
N_2 (R=2.068 au)	[445×841/200]	−108.993 825 634	−108.993 825 634 82

Table A.8: Total energies of the He, Be and Ne atoms calculated using various combinations of local exchange (LDA and B88) and correlation potentials (LYP and VWN). Algebraic results of Johnson, Gill and Pople [**?**] (denoted FB) are compared with the corresponding values obtained within the finite difference method (FD).

system	HF	LDA	LDA+VWN	LDA+LYP	B88	B88+VWN	B88+LYP
He							
FB	2.8552	2.7146	2.8267	2.7582	2.8540	2.9671	2.8978
FD	2.861680	2.723640	2.833886	2.767056	2.861725	2.972987	2.905317
Be							
FB	14.5669	14.2164	14.4420	14.3119	14.5606	14.78691	14.6563
FD	14.573026	14.223291	14.445390	14.318062	14.564197	14.787469	14.659353
Ne							
FB	128.4744	127.3950	128.1419	127.7777	128.4964	129.2442	128.6262
FD	128.547098	127.49074	128.228894	127.873286	128.587350	129.326586	128.970274

Table A.9: Total (absolute) energies of the Be and Ne atoms calculated using LDA, B88 and SCα-LDA potentials within the finite difference method as modified by Karasiev and Ludenia (FD-KL) [**?**] (note a typo in the LDA energy for the Be atom in Table II of their paper) and the present author (FD).

system	HF	LDA	B88	SCα-LDA
Be				
FD-KL		14.2233	14.5664	14.5707
FD	14.573026	14.223291	14.564244	14.570693
Ne				
FD-KL	128.5471	127.4907	128.5901	128.5322
FD	128.547098	127.490741	128.587350	128.533177

Table A.10: Exchange (absolute) energies of the Be and Ne atoms calculated using LDA, B88 and SCα-LDA potentials within the finite difference method as modified by Karasiev and Ludenia (FD-KL) [**?**] and the present author (FD).

system	HF	LDA	B88	SCα-LDA
Be				
FD-KL	2.667	2.278	2.652	2.663
FD	2.666914	2.277843	2.684667	2.663346
Ne				
FD-KL	12.108	10.937	12.086	12.065
FD	12.108351	10.937090	12.139002	12.065332

Table A.11: Electrical properties of the FH molecule calculated by means of the finite field on a [451 × 877/200] grid using the data from the upper part of the table. μ_z, α_{zz}, etc. denote the z-components of the total dipole moment, polarizability, etc. with respect to the centre of mass, while E_T, μ_z^e and Θ_{zz}^e denote the total energy and electrical dipole and quadrupole moments for a given field strength. Entries with Δ show the properties when the raw data are modified by a relative error 10^{-12}.

field strength	E_T	μ_z^e	Θ_{zz}^e
-0.0002	-100.070 823 358 990	-0.104 967 386 574 450	-1.044 975 755 481 64
-0.0001	-100.070 812 891 021	-0.104 391 834 078 358	-1.044 577 910 264 44
0.0	-100.070 802 480 605	-0.103 816 366 336 909	-1.044 180 598 585 64
+0.0001	-100.070 792 127 745	-0.103 240 983 076 439	-1.043 783 820 062 32
+0.0002	-100.070 781 832 421	-0.102 665 684 024 677	-1.043 387 574 315 97
μ_z	0.755 983 631 461 119	0.756 075 857 950 02	
$\mu_z + \Delta$	0.755 982 964 308 859	0.756 075 857 950 78	
α_{zz}	5.755 839 419 900 136	5.754 254 554 649 43	
$\alpha_{zz} + \Delta$	5.769 182 465 087 396	5.754 254 555 345 37	
β_{zzz}	-8.085 976 332 949 940	-8.448 086 128 802 03	
$\beta_{zzz} + \Delta$	91.986 862 571 502 570	-8.448 100 082 570 72	
γ_{zzzz}		272.967 398 684 543	
$\gamma_{zzzz} + \Delta$		272.862 996 086 865	
$A_{z,zz}$			3.970 450 376 067 36
$A_{z,zz} + \Delta$			3.970 450 383 032 16
$B_{zz,zz}$			-53.315 512 212 511 4
$B_{zz,zz} + \Delta$			-53.315 651 508 493 5

Table A.12: Dipole moments, polarizabilities and hyperpolarizabilities (in au) for the FH molecule from finite difference Hartree-Fock calculations performed on a [451×877/200] grid as a function of the internuclear distance (R_{FH}) [**?**].

R_{FH}	μ_z	α_{zz}	β_{zzz}	γ_{zzzz}	$A_{z,zz}$	$B_{zz,zz}$
1.5000	0.664 944 721 966	4.650 181 3	−3.950 18	178.2	1.992 651	−33.312 3
1.6000	0.703 241 445 779	5.084 822 2	−5.556 00	177.2	2.735 080	−40.602 4
1.7000	0.742 834 220 524	5.578 450 0	−7.640 36	247.5	3.636 170	−49.805 2
1.7328	0.756 075 857 946	5.754 254 6	−8.448 09	273.0	3.970 450	−53.315 5
1.8000	0.783 567 762 981	6.137 247 9	−10.314 73	311.9	4.720 885	−61.365 2
1.9000	0.825 315 757 659	6.767 259 9	−13.689 27	374.7	6.015 908	−75.771 0
2.0000	0.867 979 378 698	7.474 265 9	−17.886 06	456.5	7.549 393	−93.575 9
2.1000	0.911 482 614 182	8.263 677 7	−23.025 59	548.7	9.350 725	−115.375 2
2.2000	0.955 766 163 516	9.140 458 0	−29.221 11	655.5	11.450 279	−141.793 6

Table A.13: Electrical properties of the N_2 molecule (R=2.07432 bohr) calculated by means of the finite field on a [643 × 1261/250] grid using the data from the upper part of the table. μ_z, α_{zz}, etc. denote the z-components of the total dipole moment, polarizability, etc. with respect to the centre of mass while E_T, μ_z^e and Θ_{zz}^e denote the total energy and electrical dipole and quadrupole moments for a give field strength. Entries with Δ show the properties when the raw data are modified by a relative error of 4×10^{-14}, 3×10^{-9} and 2×10^{-14} for the energy, dipole moment and quadrupole moment, respectively.

field strength	E_T	μ_z^e	Θ_{zz}^e
-0.002	-108.993 203 207 341	-0.030 061 943 076 783	-15.991 059 035 127
-0.001	-108.993 180 661 183	-0.015 030 571 406 828	-15.990 794 227 794
0.0	-108.993 173 145 936	-0.000 000 000 000 027	-15.990 705 975 670
+0.001	-108.993 180 661 182	0.015 030 571 408 096	-15.990 794 227 794
+0.002	-108.993 203 207 337	0.030 061 942 998 232	-15.991 059 035 132
μ_z	-0.000 000 000 280 664	0.756 075 857 950 02	
$\mu_z + \Delta$	-0.000 000 003 407 052	0.756 075 857 950 78	
α_{zz}	15.030 425 559 577 527 67	15.030 438 037 031 0	
$\alpha_{zz} + \Delta$	15.030 431 812 353 601 4	15.030 438 063 214 3	
β_{zzz}	-0.001 335 820 343 229	0.000 008 302 469 534	
$\beta_{zzz} + \Delta$	0.003 353 761 712 788	-0.000 044 063 158 215	
γ_{zzzz}		800.222 583 420 898	
$\gamma_{zzzz} + \Delta$		800.183 308 998 642	
$A_{z,zz}$			0.000 000 000 707 878
$A_{z,zz} + \Delta$			0.000 000 000 909 199
$B_{zz,zz}$			-176.495 752 138 035 783
$B_{zz,zz} + \Delta$			-176.495 752 540 676 648

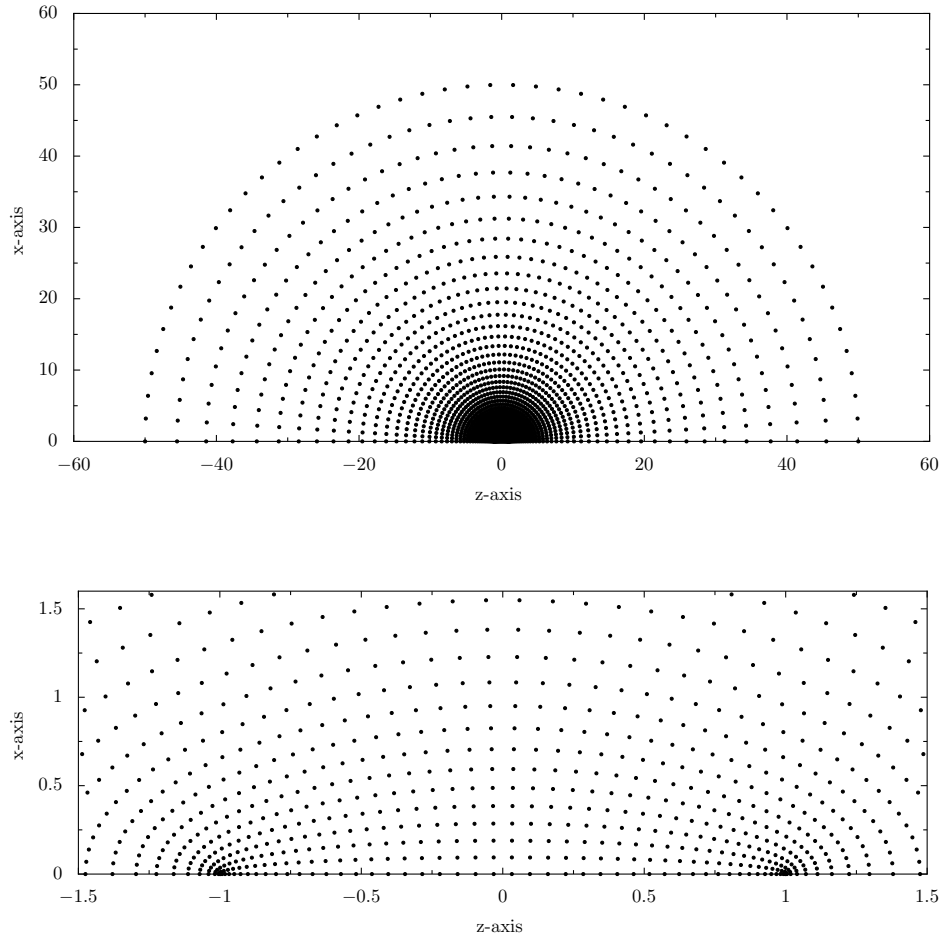

Figure A.1: Distribution of grid points in the $z-item$ plane corresponding to the uniform distribution in (ν, μ) variables on a [50×50/50] grid. The lower plot is a close-up of the region around the A and B nuclei, i.e. around (-1,0) and (1,0) points.

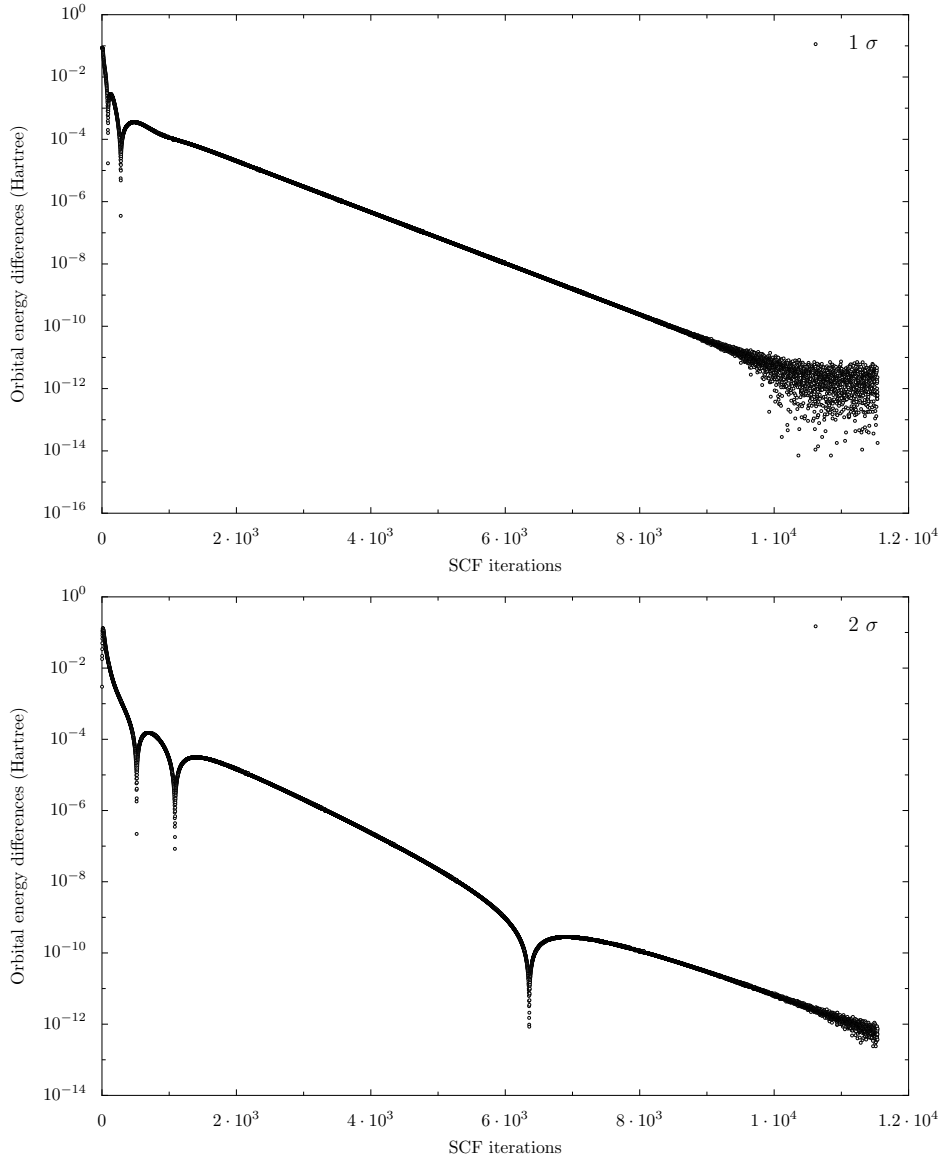

Figure A.2: Convergence patterns of 1 σ and 2 σ FH orbitals discretized on a [451×877/200] grid for suboptimal overrelaxation parameters: $\omega_{orb} = 1.65$, $\omega_{pot} = 1.68$.

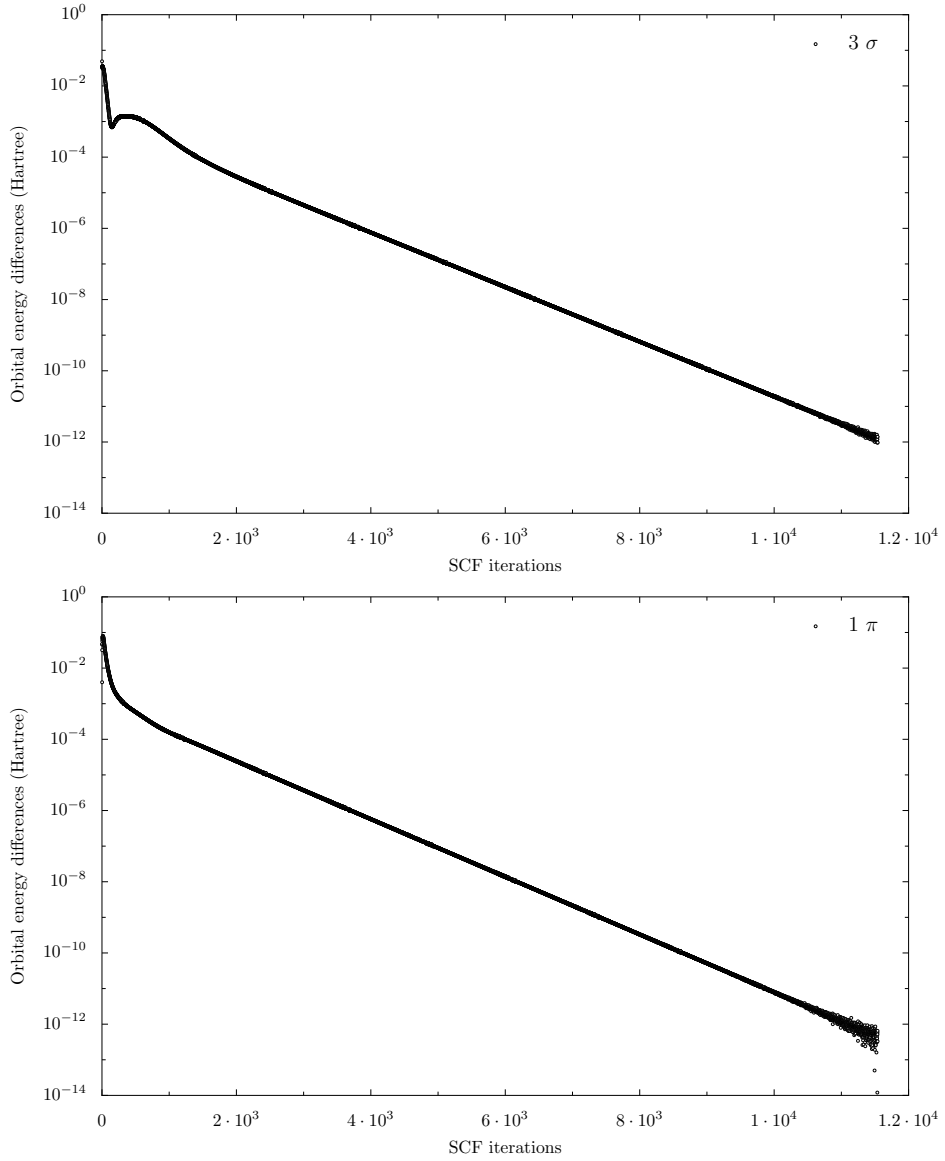

Figure A.3: Convergence patterns of 3 σ and 1 π FH orbitals discretized on a [451×877/200] grid for suboptimal overrelaxation parameters: $\omega_{orb} = 1.65$, $\omega_{pot} = 1.68$.

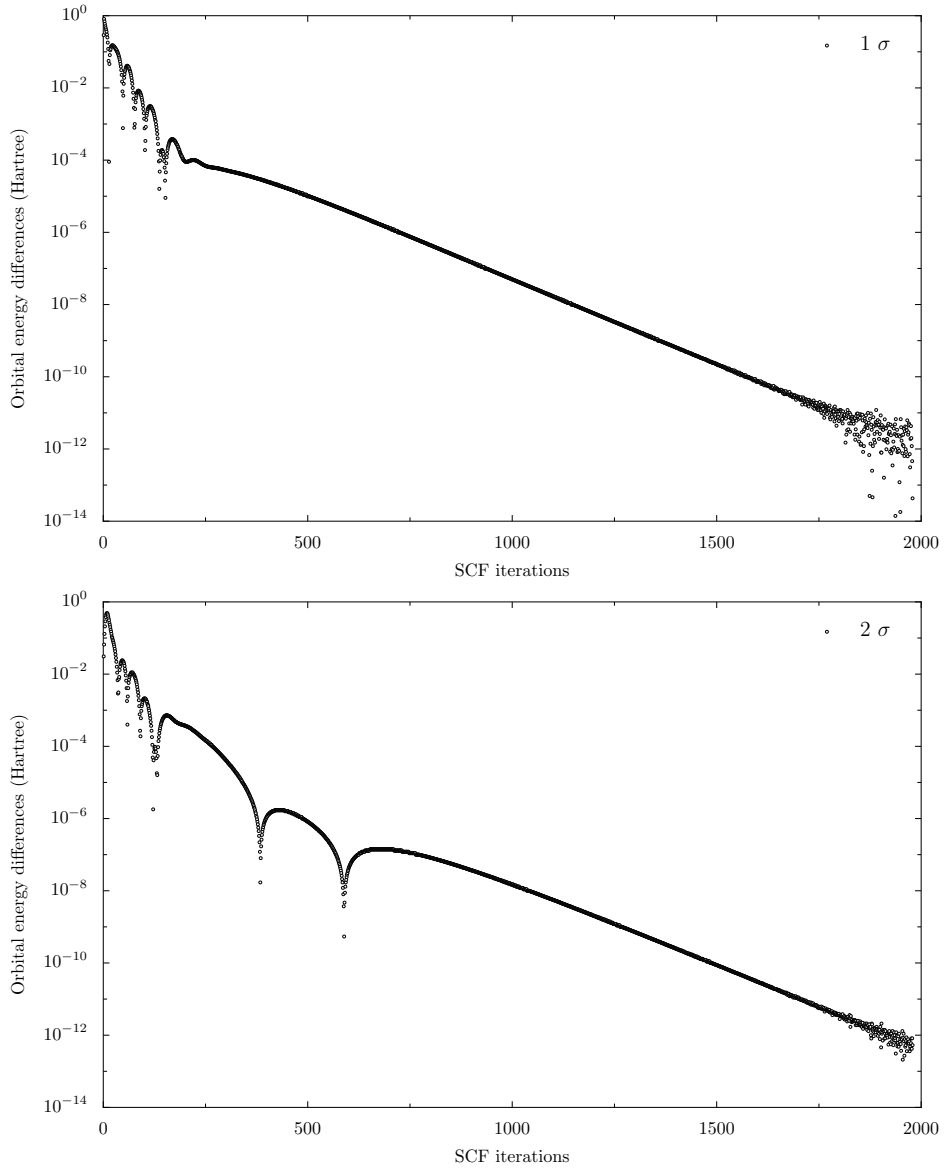

Figure A.4: Convergence patterns of 1 σ and 2 σ FH orbitals discretized on a [451×877/200] grid for near optimal overrelaxation parameters: $\omega_{orb} = 1.950$, $\omega_{pot} = 1.989$.

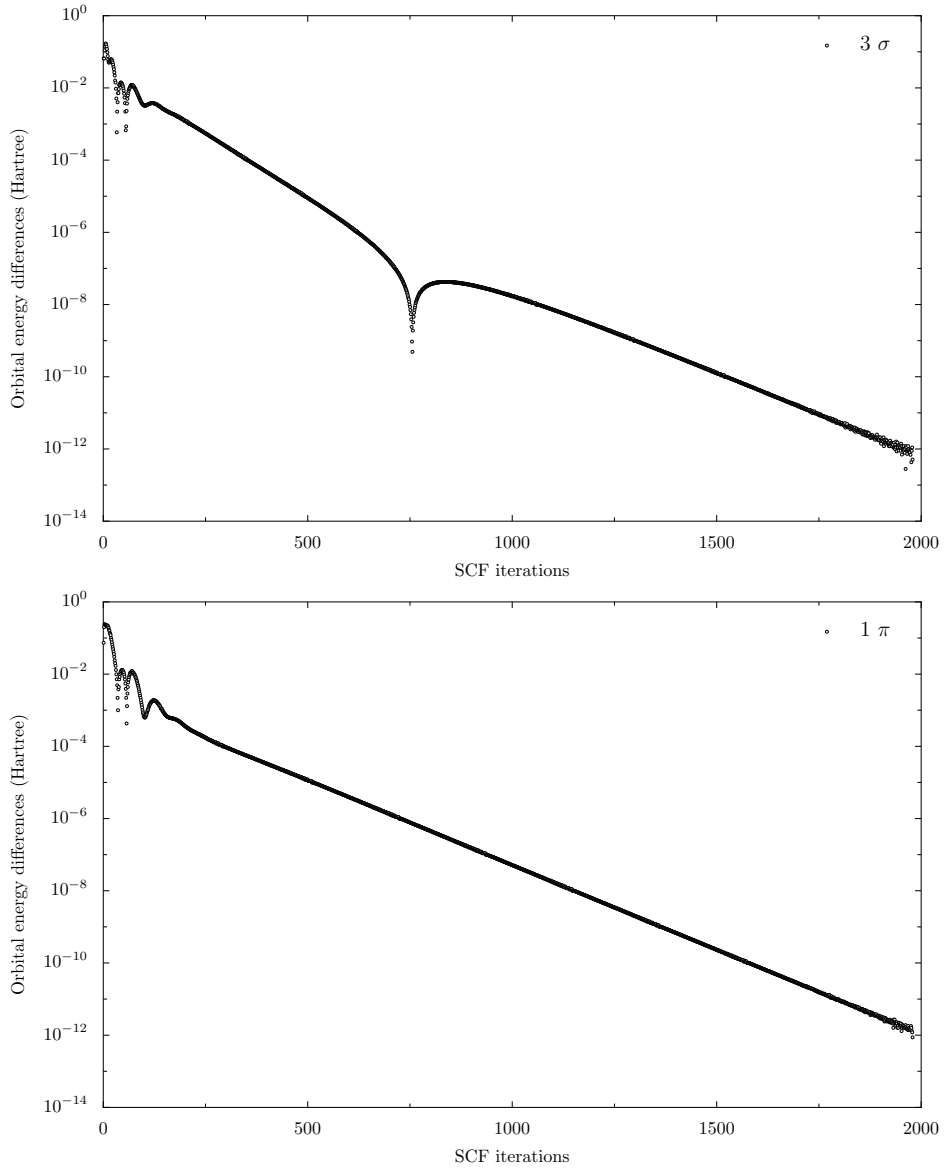

Figure A.5: Convergence patterns of 3 σ and 1 π FH orbitals discretized on a [451×877/200] grid for near optimal overrelaxation parameters: $\omega_{orb} = 1.950$, $\omega_{pot} = 1.989$.

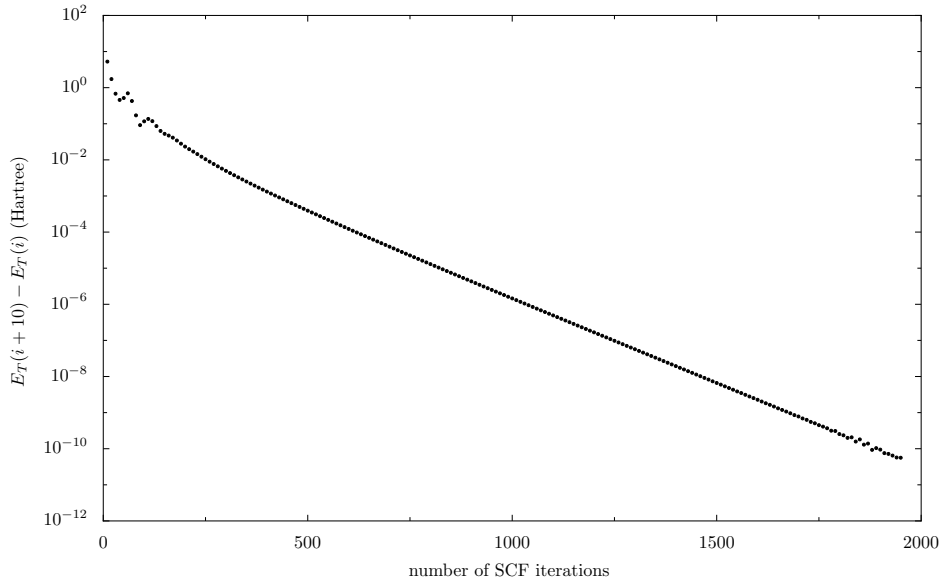

Figure A.6: Convergence pattern of the total HF energy (E_T) for the FH molecule discretized on a [451×877/200] grid for near optimal overrelaxation parameters: $\omega_{orb} = 1.950$, $\omega_{pot} = 1.989$. The convergence is measured by calculating the total energy differences every tenth SCF iteration.

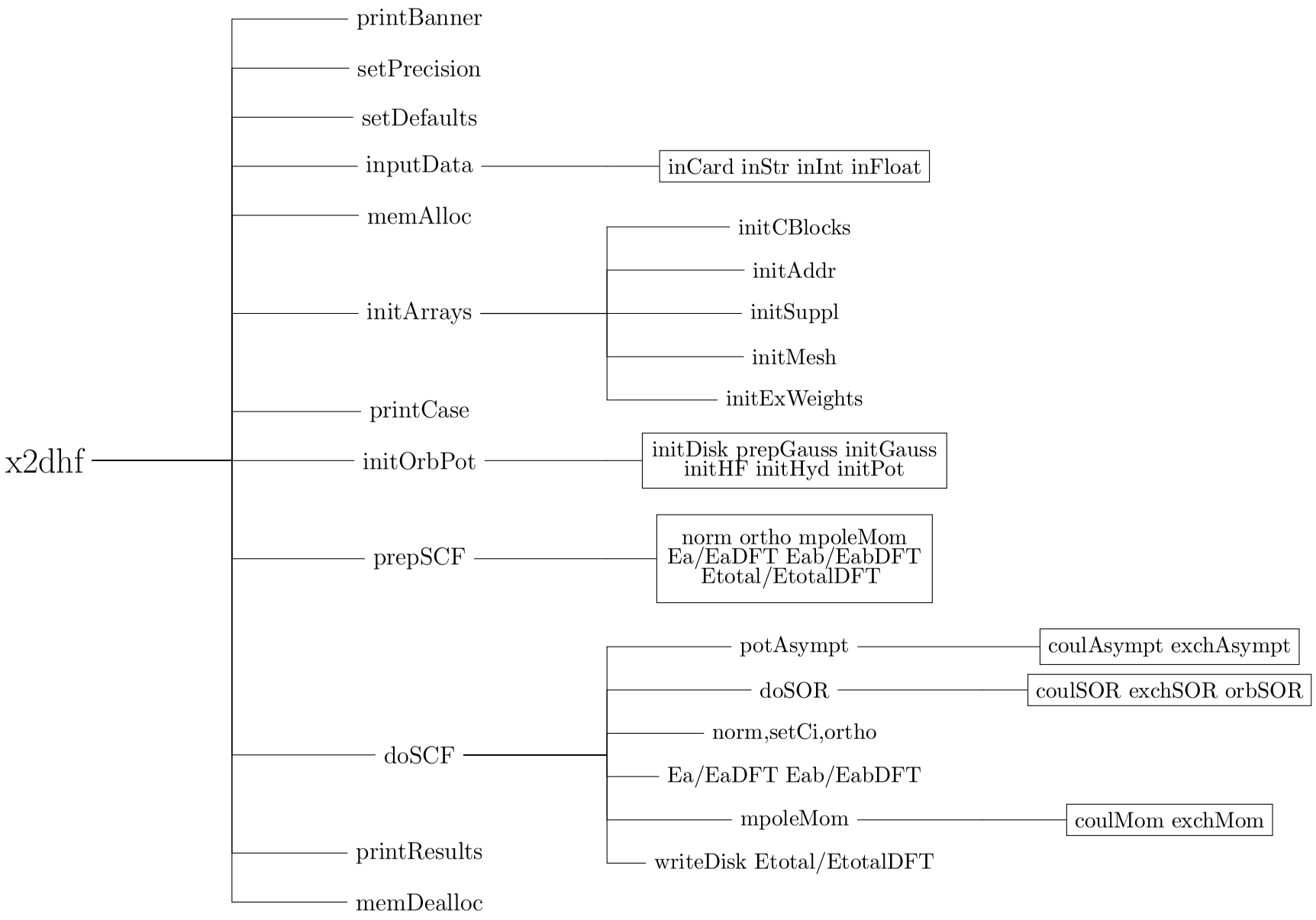

Figure A.7: Main x2dhf routine and its call tree

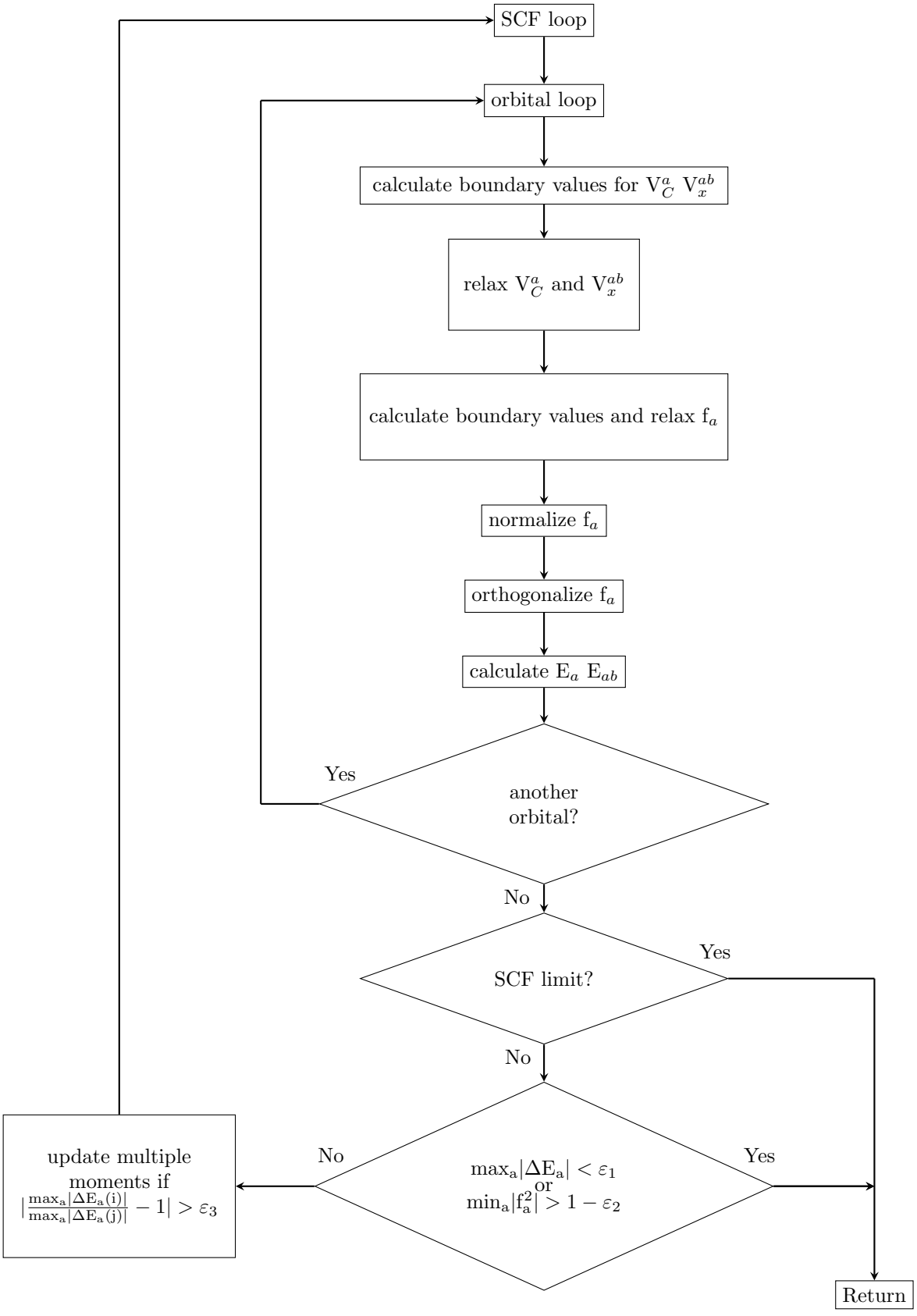

Figure A.8: SCF flowchart

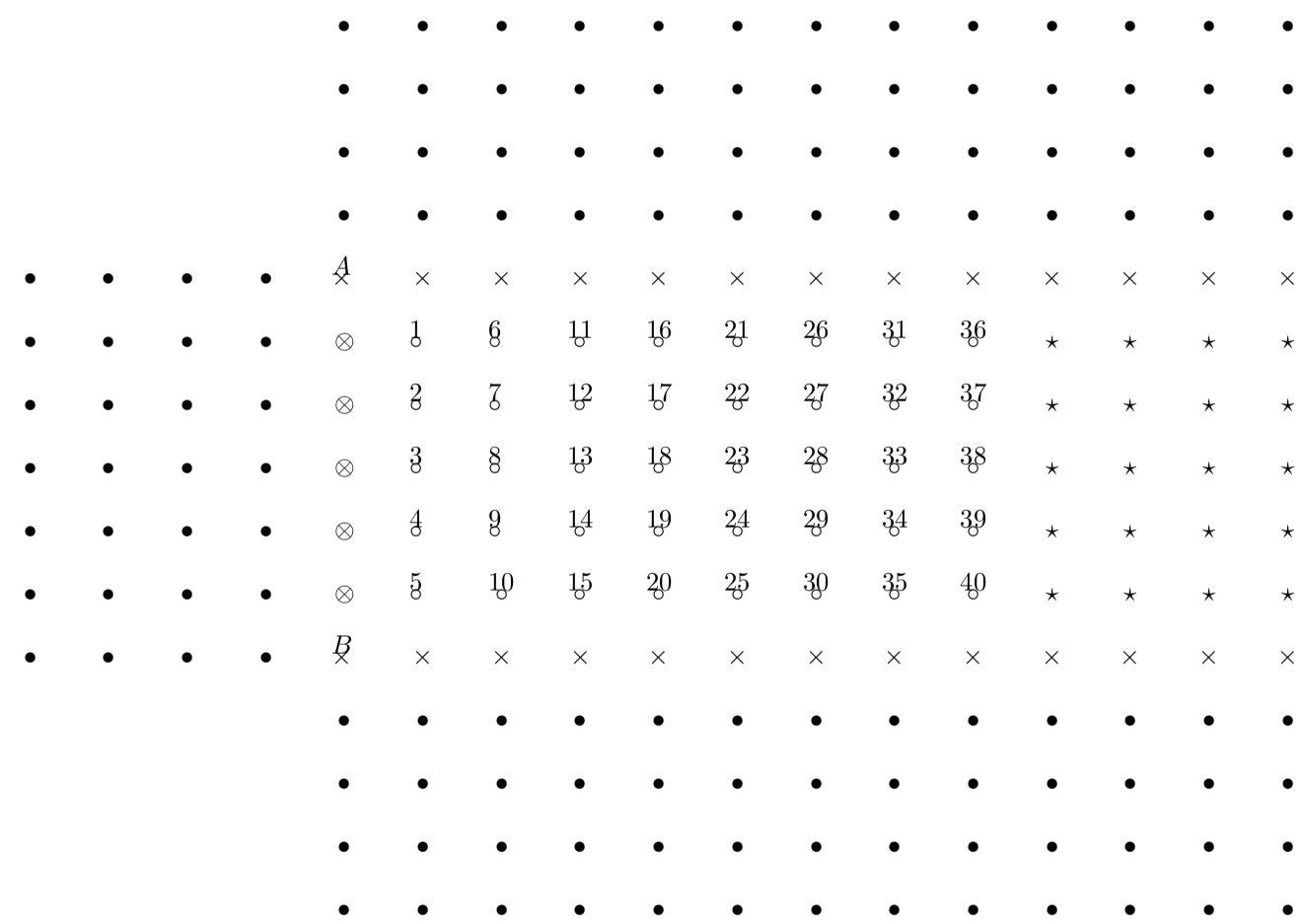

Figure A.9: Column-wise type ordering of mesh points. μ coordinate increases horizontally from left to rigth and ν vertically, e.i. the boundary points $(0, 1)$ and $(\pi, 1)$ correspond to the position of the nuclei A and B, respectively.

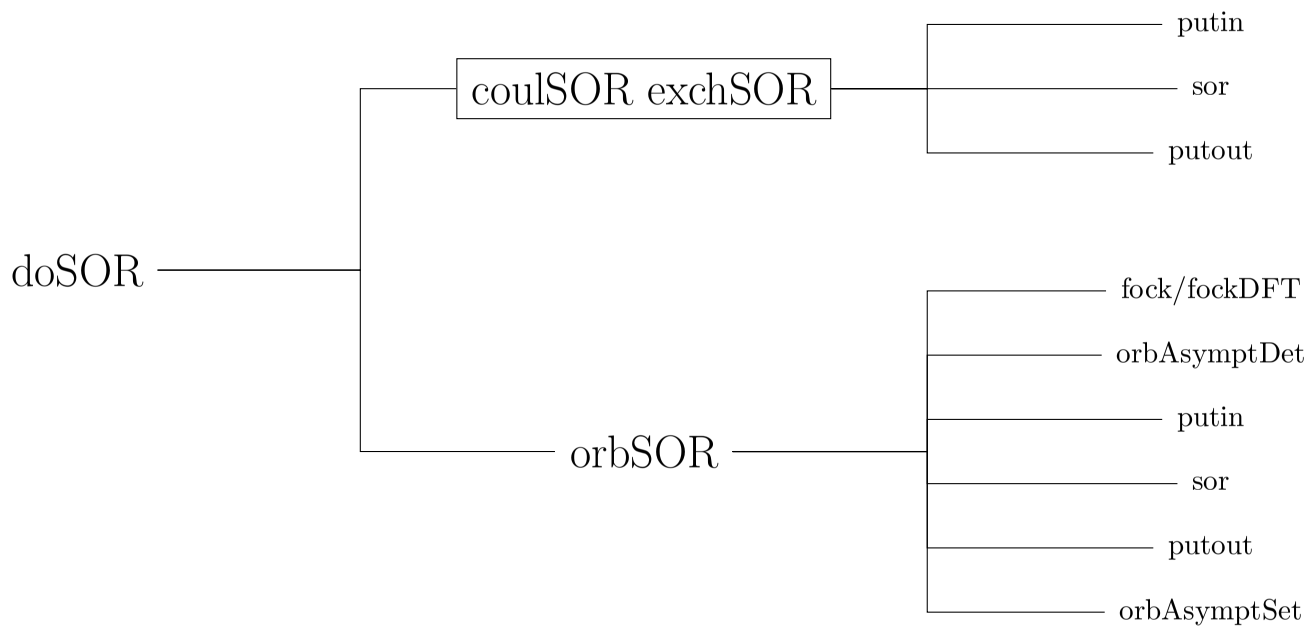

Figure A.10: `doSOR` routine and its call tree. If necesssry, `coulMCSOR`, `exchMCSOR`, `orbMCSOR` and `mcsor` variants of the routines are used.

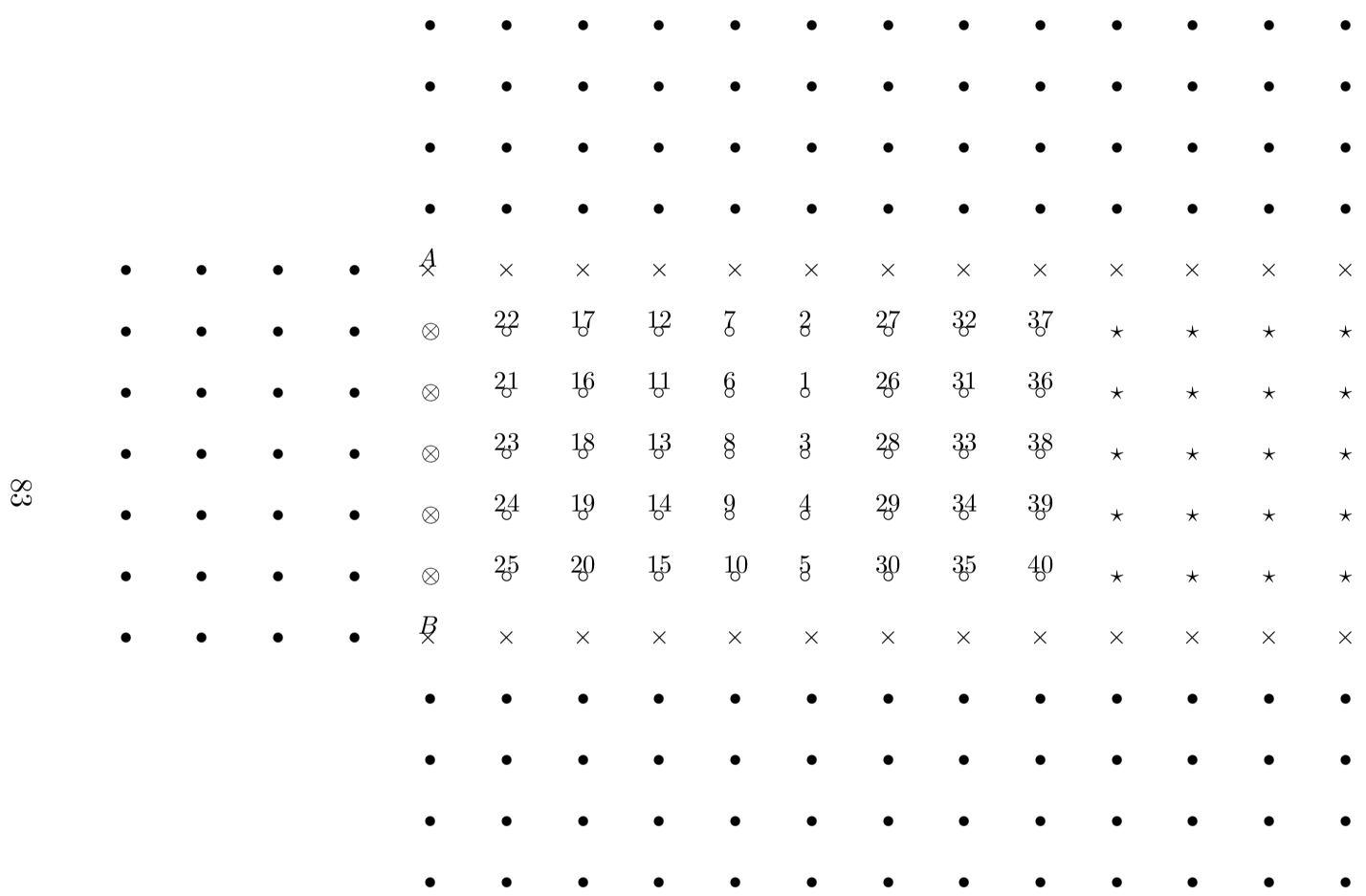

Figure A.11: 'Middle' type ordering of mesh points. μ coordinate increases horizontally from left to rigth and ν vertically, i.e. the boundary points $(0, 1)$ and $(\pi, 1)$ correspond to the position of the nuclei A and B, respectively.

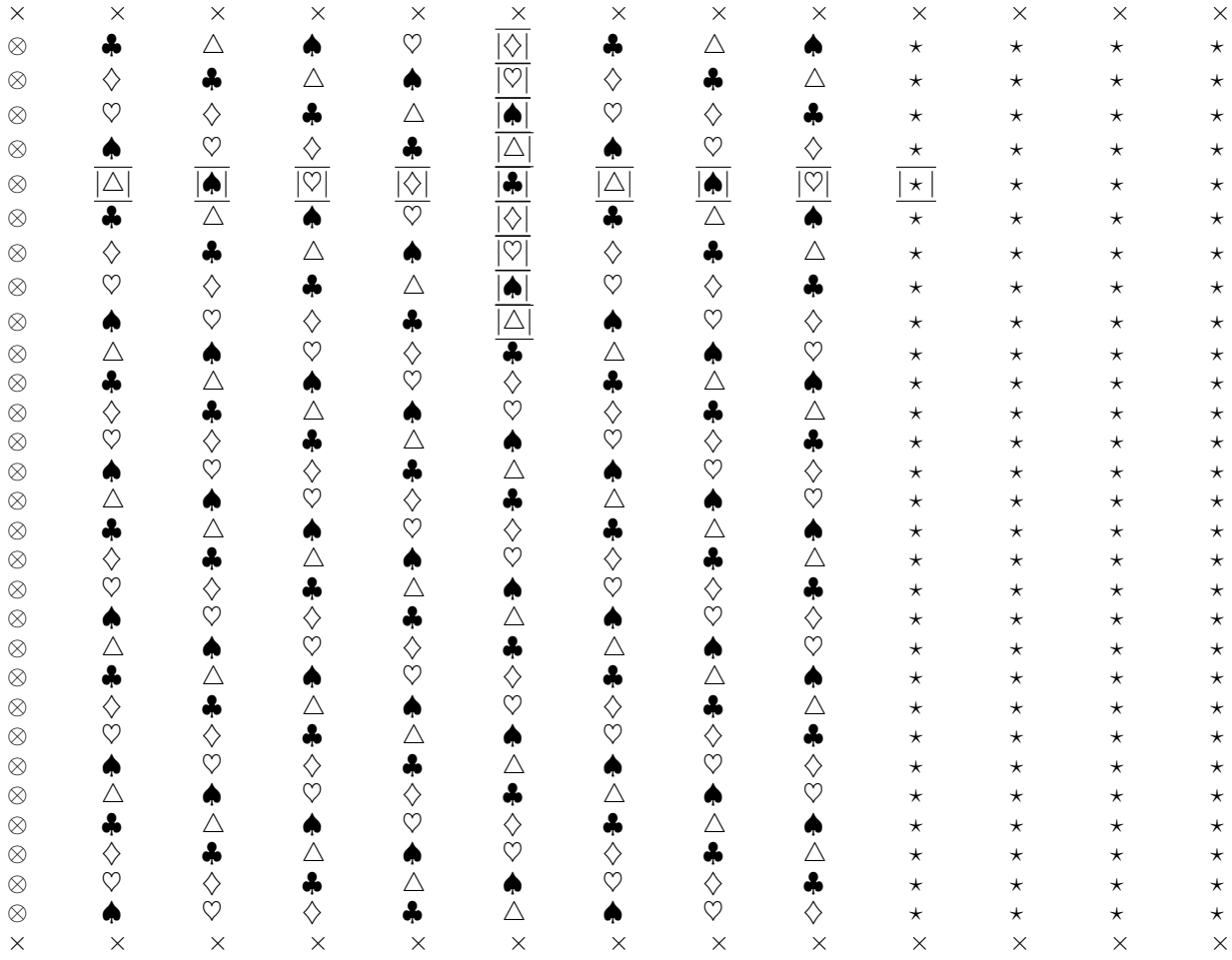

Figure A.12: Colouring of mesh points for the MCSOR method and [31×13] grid when 17-point cross-like stencil is used for discretization.